Environment International 137 (2020) 105517

Contents lists available at ScienceDirect

Environment International

journal homepage: www.elsevier.com/locate/envint

Large-scale monitoring and ecological risk assessment of persistent toxic substances in riverine, estuarine, and coastal sediments of the Yellow and Bohai seas

Seo Joon Yoon[a], Seongjin Hong[b], Seonju Kim[a], Jongmin Lee[a], Taewoo Kim[a], Beomgi Kim[a], Bong-Oh Kwon[a], Yunqiao Zhou[c], Bin Shi[c], Peng Liu[d], Wenyou Hu[d], Biao Huang[d], Tieyu Wang[c,*], Jong Seong Khim[a,*]

[a] School of Earth and Environmental Sciences & Research Institute of Oceanography, Seoul National University, Seoul 08826, Republic of Korea
[b] Department of Ocean Environmental Sciences, Chungnam National University, Daejeon 34134, Republic of Korea
[c] State Key Lab of Urban and Regional Ecology, Research Center for Eco-Environmental Sciences, Chinese Academy of Sciences, Beijing, 100085, China
[d] Key Laboratory of Soil Environment and Pollution Remediation, Institute of Soil Science, Chinese Academy of Sciences, Nanjing, China

ARTICLE INFO

Handling Editor: Adrian Covaci

Keywords:
Coastal pollution
PAHs
Alkylphenols
Styrene oligomers
Ecological risk assessment
East Asia

ABSTRACT

The Yellow and Bohai seas comprise one of the most rapidly developing regions in the world, but efforts to assess coastal pollution by persistent toxic substances (PTSs) on wide spatial scale are lacking. The present study aimed to (1) measure the concentrations of PTSs, such as polycyclic aromatic hydrocarbons (PAHs), alkylphenols (APs), and styrene oligomers (SOs) via large-scale sediment monitoring (total of 125 locations), (2) assess potential ecological risk of PTSs in sediments to coastal ecosystems, (3) estimate various sources and fresh inputs of PTSs, (4) determine distribution patterns of PTSs by human activities and land-use type, and (5) address decadal (2008–2018) changes in distributions of PTSs. The high concentrations of PAHs [> 7000 ng g^{-1} dry weight (dw)] in sediments were detected in Nantong in the Yellow Sea of China (YSC) and Huludao and Qinhuangdao in the Bohai Sea (BS), whereas lesser concentrations (< 200 ng g^{-1} dw) were detected in the Yellow Sea of Korea (YSK). We found relatively high concentrations of sedimentary APs and SOs in Nantong, Huludao, and Qinhuangdao from the YSC and BS regions, but corresponding concentrations were generally below < 100 ng g^{-1} dw in other locations. Concentrations of PAHs at 38 locations (30% of YSC and BS) posed a potential risk to aquatic ecosystems, whereas relatively low risk concentrations occurred in all locations of YSK. The main source of PAHs (concentrated in YSC and BS) were by-products of diesel and gasoline combustion (42% of total concentration), whereas biomass combustion (24%) dominated in YSK. Fresh inputs of PTSs indicated that the generation and use of PTSs continue across all regions and locations. Among PTSs, concentrations of PAHs were significantly associated with location ($p < 0.05$) relative to land-use within a given region, whereas concentrations of APs and SOs showed no significant relationships ($p > 0.05$) among or within regions. Over time, concentrations of PAHs have generally declined, but sediment contamination has increased at some locations in China, with sources shifting from a mixture of PAHs types to those linked to diesel and gasoline combustion. Additional studies are needed on the fate and potential ecological risk posed by certain PTSs in hotspots. This is one of the first efforts providing backgrounds on PTS pollution in the large marine ecosystem of the Yellow and Bohai seas.

1. Introduction

Persistent toxic substances (PTSs) are ubiquitous contaminants in various environmental matrices, originating from numerous sources, and are transported via a variety of mechanisms and pathways to the marine environment. The fate and impacts of typical PTSs are well known; they tend to accumulate in sediments after sinking with organic matter, where they exert adverse impacts to aquatic ecosystems (Hong

* Corresponding authors.
E-mail addresses: seojoonyoon@snu.ac.kr (S.J. Yoon), hongseongjin@cnu.ac.kr (S. Hong), sjhn2000@snu.ac.kr (S. Kim), jongmin8358@snu.ac.kr (J. Lee), taewoo0716@snu.ac.kr (T. Kim), bk1221@snu.ac.kr (B. Kim), bongkwon@snu.ac.kr (B.-O. Kwon), zhouyunqiao@163.com (Y. Zhou), binshi@rcees.ac.cn (B. Shi), pliu@issas.ac.cn (P. Liu), wyhu@issas.ac.cn (W. Hu), bhuang@issas.ac.cn (B. Huang), wangtieyu@163.com (T. Wang), jskocean@snu.ac.kr (J.S. Khim).

https://doi.org/10.1016/j.envint.2020.105517
Received 13 October 2019; Received in revised form 2 January 2020; Accepted 20 January 2020

et al., 2012a; Lee et al., 2018; Khim et al., 2018a). Polycyclic aromatic hydrocarbons (PAHs), alkylphenol (APs), and styrene oligomers (SOs) constitute classic and emerging PTSs. Originating from anthropogenic activities and natural sources, PTSs are widely distributed in benthic environments (Hong et al., 2016; Lee et al., 2017a,b; Yoon et al., 2017) where they pose potentially significant ecological threats to aquatic organisms.

PTSs are hydrophobic and hydrophilic organic pollutants with fused benzene rings. PAHs with 2–6 fused benzene rings are intentionally or unintentionally released from a variety of sources, including incompletely combusted fossil fuels and biomass, spilled crude or refined oil, and smelted metals (Lin and Zhu, 2004; Moon et al., 2006; Ghosh et al., 2015). PAHs spread through atmospheric deposition, wastewater streams, and industrial effluents but their fate vary depending on the multiple potential pathways they can follow. PAHs are a major contaminant and adversely affect aquatic ecosystems at concentrations above thresholds values (Engraff et al., 2011). APs are a widely used class of nonionic surfactants, with many industrial and household applications (White et al., 1994). Nonylphenol ethoxylates (NPEOs) and octylphenol ethoxylates (OPEOs) are the most common alkylphenol ethoxylates, both of which degrade via microbial and photochemical processes to nonylphenols (NPs) and octylphenol (OP), respectively (Li et al., 2013). APs are harmful endocrine disruptors and function to adversely stimulate feminization, reduce growth rates (Chen and Yen, 2013), inhibit reproduction, and cause neurological, and immunological problems (Giesy and Snyder, 1998). SOs, recently emerging as contaminants in sediments, have been reported from inland creeks (Hong et al., 2016), from estuary and coastal areas in a few regions (Yoon et al., 2019), and from sandy beaches worldwide (Kwon et al., 2015). SOs are generated from the degradation of polystyrene at high temperatures (240–300 °C) (Kwon et al., 2014) and have been reported to harm aquatic biota by causing genetic and reproductive toxicities (Ohyama et al., 2001; Tatarazako et al., 2002). Although SOs have been recently recognized as a new class of PTSs, widespread distribution in China is unknown.

The Yellow Sea (YS) and Bohai Sea (BS) are wide but semi-enclosed seas with a complex coastline that slowly exchanges waterbody encompassing many large rivers and estuaries (Chen, 2009). These two seas together are part of the Yellow Sea Large Marine Ecosystem (YSLME), which is one of 66 large marine ecosystem (LMEs) worldwide. Among these 66 LMEs, YSLME encompasses the most strong marine industrial activity being associated with the severe PTSs pollution in the very region [Table S1; Supplementary Materials (S)] (Hoagland and Jin, 2006)

The YS and BS are about 470,000 km^2 in size and is bordered by three countries: South Korea, North Korea, and China. South Korea and China are undergoing massive industrial and municipal development along the coasts of the YSLME and so those human activities are likely responsible for the increase in coastal pollution by PTSs. It has been reported that many anthropogenic pollutants have accumulated in the sediments of YS and BS (Khim et al., 2018b), but majority of the previous studies have either only reported pollution by some PTSs or in limited areas along the YSLME coasts (Meng et al., 2017). However, from these limited studies, most pollution indices for the YSLME exhibit high values and so we expect that the YSLME is severely contaminated.

Economic development intensifies land-use practices, which in turn negatively impact aquatic ecosystems. Coastal aquatic ecosystems are altered and contaminated by coastal development and discharges of land-driven pollutants from surrounding activities are a global problem (Saxena et al., 2015). The major factors responsible for sediment pollution in estuaries and coastal areas worldwide are due to changes in land-use associated with anthropogenic activities and lack of procedures to contain runoff (Karstens et al., 2016; Liu et al., 2017). In fact, some chemical contaminants, such as metals and PTSs identified in coastal sediments can be directly linked to land-use type (Kimbrough and Dickhut, 2006). Therefore, characterization of coastal land-use is fundamental for addressing sources of coastal pollution of PTSs.

In the present study, we surveyed 125 locations, representing most coasts of the Yellow and Bohai seas to (1) measure concentrations of PTSs in sediment, specifically targeting selected chemicals of PAHs, APs, and SOs, (2) assess potential ecological risks posed by the PTSs, (3) identify sources of targeted contaminants, especially via freshwater inputs, (4) characterize spatial distribution patterns linked to land-use types, and (5) evaluate long-term changes (past 10 y) in sedimentary contamination of selected PTSs. Results of the present study would provide baseline information on PTSs contamination, such as point sources and hotspots, in a large marine ecosystem of the Yellow and Bohai seas and provide scientific data for informed decision-making and environmental management of the given coastal ecosystem.

2. Materials and methods

2.1. Study area and sampling

The present study focused on most coasts of the YSLME, encompassing both South Korea and China, because both countries have high socioeconomic dependency on the coast. Several metroplexes have grown along the coastline in South Korea (Seoul, Incheon, Asan, Gunsan, and Mokpo) and China (Beijing, Tianjin, Dalian, Huludao, Qinhuangdao, Weifang, Yantai, Qingdao, and Nantong). About 300 million people currently live near the coastline of the YS and BS, and population growth and development continue unabated (National Bureau of Statistics, 2018; KOSIS, 2018). In addition, more than 60 rivers flow to the YS and BS, including major rivers of South Korea (Han, Geum, and Yeongsan) and China (Liaohe, Haihe, Yellow, Dagu, and Guanhe), all of which convey organic contaminants to coastal waters (Wang et al., 2015; Zhen et al., 2016; Jeon et al., 2017). The study's data represent inputs from all the large cities and major rivers along the coast of the YSLME.

We employed a comprehensive field survey by collecting freshwater and saltwater sediments in the major rivers, estuaries, and some intertidal areas along the entire coasts of the YSLME. Four teams simultaneously conducted extensive field sampling for about three weeks in June–July 2018 in China and South Korea, in order to collect all the samples within a short period. We surveyed 125 locations in four provinces in South Korea (Gyeonggi, Chungnam, Jeonbuk, and Jeonnam) and four provinces in China (Liaoning, Hebei, Shandong, and Jiangsu), and one city in China (Tianjin) (Fig. 1). Detailed information on sampled locations, including geographic location and basic water quality parameters, are provided in Table S2. In brief, the land-use types adjacent to the 125 sampled locations varied widely. There were 21 industrial locations, 20 municipal locations, 38 agriculture locations, 9 beaches, 6 aquaculture locations, 5 salterns, and 26 barren lands (unused area). We assigned land-use types based on dominant surrounding activity at the time of sampling and supplemented our records by referring to the previous studies that provided data on land-use type at the same locations (Jiao et al., 2012; Hong et al., 2012b). We collected surface sediment samples using stainless steel devices (from top 2 cm), consisting of three replicate at each site, and then stored the samples in pre-cleaned glass bottles. We stored all collected sediment samples in a cooler at −20 °C for transportation to a laboratory.

2.2. Chemicals and reagents

We obtained standards for target PTSs from ChemService (West Chester, PA), which included 16 PAHs, including naphthalene (Na), acenaphthylene (Acl), acenaphthene (Ace), fluorene (Flu), phenanthrene (Phe), anthracene (Ant), fluoranthene (Fl), pyrene (Py), benzo[*a*]anthracene (BaA), chrysene (Chr), benzo[*b*]fluoranthene (BbF), benzo[*k*]fluoranthene (BkF), benzo[*a*]pyrene (BaP), indeno[*1,2,3-c,d*]pyrene (IcdP), dibenz[*a,h*]anthracene (DahA), benzo[*g,h,i*]perylene (BghiP), and another 23 alkyl-PAHs. We obtained authentic standards

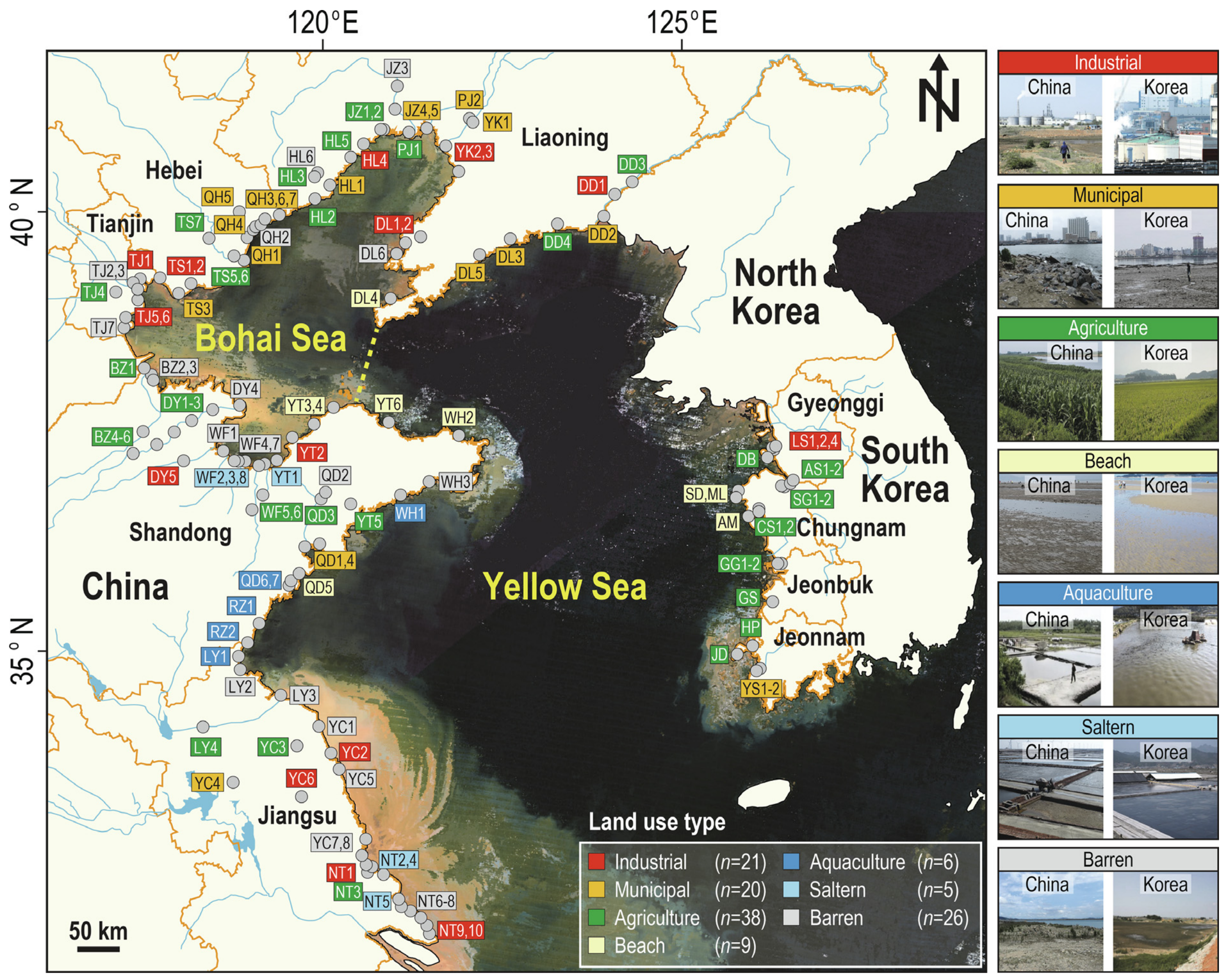

Fig. 1. Map showing the sampled locations in the Yellow and Bohai seas. The images on the right depict typical land-use types in South Korea and China (land-use classifications are based on dominant surrounding activity). (For interpretation of the references to color in this figure legend, the reader is referred to the web version of this article.)

for 6 APs and 10 SOs from Sigma-Aldrich, Wako Pure Chemical Ind. (Osaka, Japan) and Hayashi Pure Chemical Ind. (Osaka, Japan), which included 4-*tert*-octylphenol (OP), 4-*tert*-octylphenol monoethoxylate (OP1EO), 4-*tert*-octylphenol diethoxylate (OP2EO), nonylphenols (NPs), nonylphenol monoethoxylates (NP1EOs), and nonylphenol diethoxylates (NP2EOs), 1,3-diphenylpropane (SD1), *cis*-1,2-diphenylcyclobutane (SD2), 2,4-diphenyl-1-butene (SD3), *trans*-1,2-diphenylcyclobutane (SD4), 2,4,6-triphenyl-1-hexene (ST1), 1e-phenyl-4e-(1-phenylethyl)-tetralin (ST2), 1a-phenyl-4e-(1-phenylethyl)-tetralin (ST3), 1a-phenyl-4a-(1-phenylethyl)-tetralin (ST4), 1e-phenyl-4a-(1-phenylethyl)-tetralin (ST5), and 1,3,5-triphenylcyclohexane (isomer mix) (ST6). Detailed information and abbreviations for the target compounds are provided in Table S3.

2.3. PTSs analyses

In the laboratory, we prepared sediment samples for analyses of PTSs following previous methods of Khim et al. (1999) and Hong et al. (2016), with minor modifications. With a Soxhlet extractor, we extracted freeze-dried and homogenized 10 g of sediment over a 16 h period with five surrogate standards (acenaphthene-d_{10}, phenanthrene-d_{10}, chrysene-d_{12}, perylene-d_{12}, and bisphenol A-d_{16}) and 300 mL dichloromethane (DCM) (Burdick & Jackson, Muskegon, MI). Activated copper powder (Sigma Aldrich, Saint Louis, MO) was added to remove elemental sulfur. Organic extracts were then concentrated using rotary evaporators and fractionated with activated silica gel column (70–230 mesh, Sigma-Aldrich). We eluted the first fraction (F1) for PAHs and SOs with 60 mL of 20% DCM in hexane (v/v) (Burdick & Jackson). We collected the second fraction (F2) for APs with 50 mL of 60% DCM in acetone (J.T. Baker, Center valley, PA). Then, extracts were concentrated using N_2 gas flow and added 2-fluorobiphenyl as an internal standard.

Target PTSs were quantified using an Agilent 7890A gas chromatograph equipped with a mass selective detector (GC-MSD) (Agilent Technologies, Santa Clara, CA). We injected each sample onto a DB-5MS Ultra Inert fused silica capillary column (30 m × 0.25 mm i.d. × 0.25 μm film, Agilent) for chromatographic separation. Details on the instrumental conditions for PTS analyses are provided in Table S3.

Method detection limits (MDLs) were defined as standard deviations 3.707-fold of standard materials quantified seven times. Concentration ranges for MDLs were 0.27–0.90 ng g^{-1} dry weight (dw) for PAHs, 0.10–0.91 ng g^{-1} dw for APs, and 0.24–0.91 ng g^{-1} dw for SOs. The concentrations of PAHs in the procedural blank samples were all lower than those of MDLs. Recoveries for the five surrogate standards were 68–96% (mean = 80%) for acenaphthene-d_{10}, 90–121% (mean = 110%) for phenanthrene-d_{10}, 75–105% (mean = 93%) for chrysene-d_{12}, 69–98% (mean = 88%) for perylene-d_{12}, and 62–90% (mean = 78%) for bisphenol A-d_{16}. Recovery rates of the standard reference material 1944 were generally acceptable, ranging from 80% to 126% (mean = 106%) (Table S4).

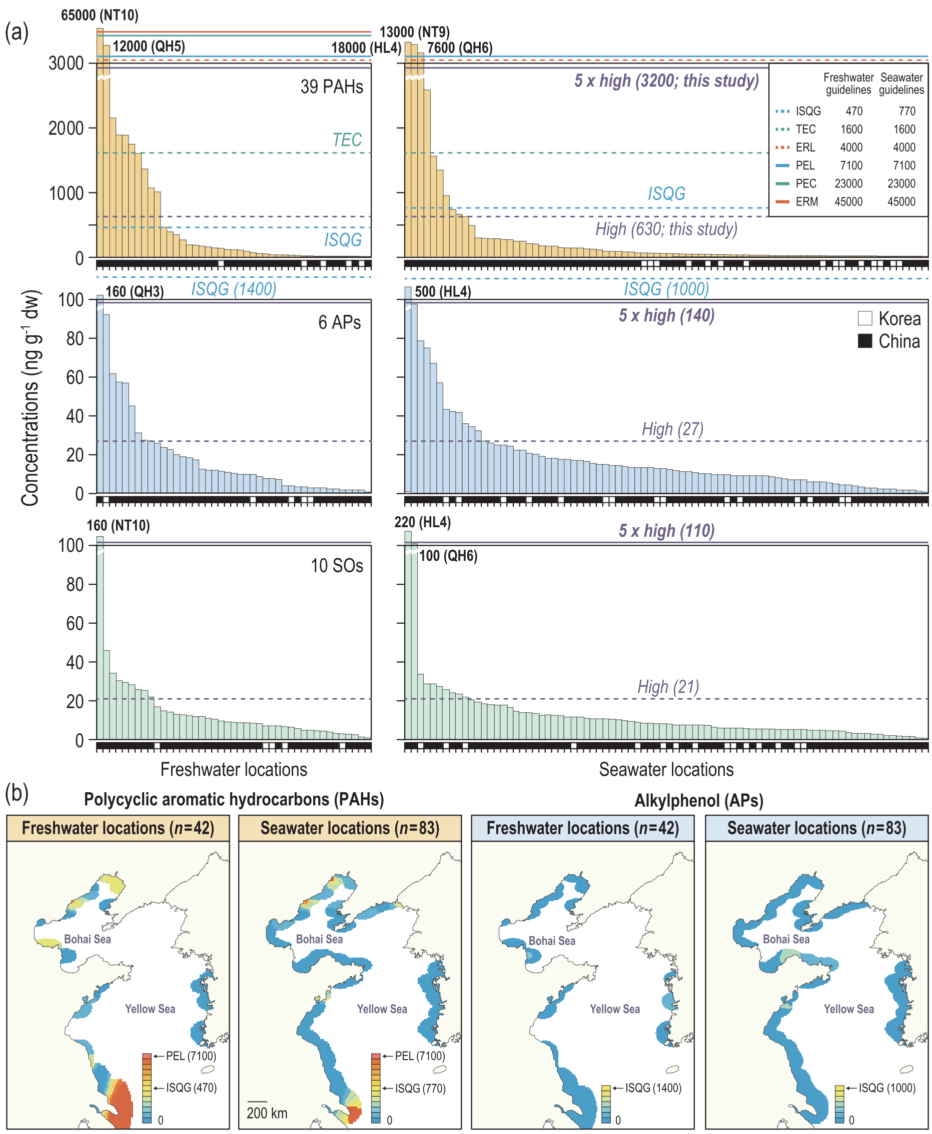

Fig. 2. Distributions of PTSs in sediments of the Yellow and Bohai Seas. Panels: (a) PAHs (n = 39), APs (n = 6), and SOs (n = 10) and (b) potential ecological risk from low (blue) to high (red) levels of contamination. High concentrations are defined as the 85th percentile of samples in this study, whereas 5-x-high concentrations are five times higher than the High concentration. Dotted and solid lines indicate existing sediment quality guidelines [(ISQG: interim sediment quality guidelines, PEL: probable effect levels (CCME, 2001; CCME, 2002); TEC and PEC: threshold and probable effect concentrations (Solberg et al., 2003); ERL and ERM: effect range low and median values (Long et al., 1995)]. (For interpretation of the references to color in this figure legend, the reader is referred to the web version of this article.)

2.4. TOC, TN, and stable isotopes analyses

To determine the grain sizes of sediments, we treated about 20 g of sediment with hydrogen peroxide before being analyzed with a Mastersizer 3000 (Malvern Panalytical, Malvern, West Midlands). We freeze-dried and homogenized sediments for analyzing total organic carbon (TOC), total nitrogen (TN), and stable isotope ratios of carbon ($\delta^{13}C$). To decalcify sediments for TOC and $\delta^{13}C$ analyses, acidified samples were acidified with 1 M HCl. Then samples were washed three times with deionized water, and freeze-dried them again. TOC, TN, and $\delta^{13}C$ were then measured with an Elemental Analyzer-Isotope Ratio Mass Spectrometer (EA-IRMS) (Elementar, Gmbh, and Hanau). All isotopic compositions were expressed as δ notation (‰) (Eq. (1)):

$$\delta^{13}C\ (‰) = [R_{sample}/R_{reference} - 1] \times 1000 \quad (1)$$

wherein R is the composition ($^{13}C/^{12}C$) of the sample and reference. We used Vienna Peedee Belemnite (VPDB) as carbon reference material and IAEA-CH-3 [International Atomic Energy Agency (IAEA), Vienna, Austria] as a standard material. The analytical errors were 0.04‰ for C estimated by IAEA working standards [CH-6 for carbon, International Atomic Energy Agency (IAEA), Vienna, Austria].

2.5. Positive matrix factorization receptor model

We employed the U.S. Environmental Protection Agency positive matrix factorization (PMF) receptor model (Ver. 5.0) to source apportion PAHs, which is a generic factorization method for quantifying the contribution of source compositions (Larsen and Baker, 2003; Norris et al., 2014). Each factor contribution and profile is drawn from minimizing the objective function Q, defined as

$$Q = \sum_{i=1}^{n} \sum_{j=1}^{m} \left[\frac{x_{ij} - \sum_{k=1}^{p} g_{ik} f_{kj}}{u_{ij}} \right]^2 \quad (2)$$

wherein u_{ij} is the uncertainty in the x_{ij} measurement, x_{ij} is the concentration of species j in sample i, p is the number of factors, g_{ik} is a relative contribution of each factor k, and f_{kj} is species profile of each source. Uncertainties (*Unc*) for each PAH relative to each MDL were calculated using either Eq. (3) or Eq. (4) (below), following PMF user guidelines. Eq. (3) was used when the concentration was less than the MDL; Eq. (4) was used when the concentration was higher than the MDL.

$$Unc = 5/6 \times MDL \quad (3)$$

$$Unc = \sqrt{(ErrorFraction \times concentration)^2 + (0.5 \times MDL)^2} \quad (4)$$

wherein the *ErrorFraction* was calculated as the standard deviation of the concentration of *j*. When the detection frequency was < 40%, Acl, Ace, Dbthio, and alkyl-PAHs were excluded. Additionally, Na was not included in the model due to possible losses of it during analysis.

2.6. Data analyses

We categorized concentrations of PTSs following methods outlined by NOAA (1991) and Daskalakis and O'Connor (1995). 'High' concentrations of PTSs were defined as the 85th percentile value among all concentrations measured. The High and five-times-High (5-x-High) concentrations in sediments of YS and BS are suggested for providing regional criteria of PTSs in sediments. Using the definition for High PTS concentrations, we categorized all locations as being High, 5-x-High, or Low (neither High nor 5-x-High). SPSS 25.0 (SPSS INC., Chicago, IL) was used to conduct statistical analyses and used non-parametric statistical analysis for data that were not normally distributed. Differences in concentrations of PTSs by land-use type and region were evaluated with the Kruskal-Wallis test and the Mann-Whitney test with Bonferroni correction. Principal Component Analysis (PCA) was performed using fourth-root transformed values of PTS concentrations and physicochemical parameters and linear regression analysis was used to understand the relationship between concentrations of PTSs and physicochemical parameters. To compare our data to guidelines of the Canadian Council of Ministers of the Environment (CCME, 2002), we converted concentrations of APs with toxic equivalency factors (TEFs) and normalized them to 1% TOC, as outlined in Section 3.2 of CCME guidelines. For the 16 PAHs provided for South Korea and China in 2008, we used data reported by Hong et al. (2012b).

3. Results and discussion

3.1. Distributions of PTSs in sediments of Yellow and Bohai seas

PAHs, APs, and SOs were detected in all sediments of the YS and BS (Fig. 2a, Table S5, and Table S6). Concentrations of PAHs in the YS and BS ranged from 6.2 to 65000 ng g^{-1} dw in sediment from freshwater locations and 2.1 to 18000 ng g^{-1} dw in sediment from seawater locations. The high concentrations exceeding 5-x-High concentration (3200 ng g^{-1} dw) were detected in both industrial (NT10, HL4, and NT9) and municipal locations (QH5 and QH6) (Table S2). In previous studies, relatively lower concentrations of PAHs had been detected (20–5700 ng g^{-1} dw) from some areas sampled in present study (Ma et al., 2001; Jiao et al., 2012; Zhang et al., 2014), despite them not having changed in their land-use designations, which suggested that these areas have been affected by increasing contamination sources.

We compared the High and 5-x-High concentration categories of our study to other defined criteria, including effect-range low (ERL) and effect-range median (ERM) concentrations defined by Long et al. (1995), threshold-effect concentrations (TEC) and probable-effect concentrations (PEC) defined by Solberg et al. (2003), and interim sediments quality guidelines (ISQG) and probable effect levels (PEL) defined by CCME (2001) (Fig. 2 and Table 1). Our High and 5-x-High concentrations were similar to the threshold effect concentration guidelines (TECs), such as ERL, TEC, and ISQG. However, both High and 5-x-High concentrations were lower than the probable effect concentration guidelines (PECs), such as ERM, PEC, and PEL. In addition, our High and 5-x-High concentrations for individual compounds were generally lower than TECs and PECs, with the exception of DbahA, which was higher than TECs and PECs, indicating input from sources specific to the Yellow and Bohai seas. Overall, regional criteria of PAHs for YS and BS were similar or lower than existing sediment quality guidelines, indicating that YS and BS were moderately contaminated by PAHs.

Concentrations of PAHs exceeding guidelines were found mainly in the Yellow Sea of China (YSC) and the BS. In the Yellow Sea of South Korea (YSK), we did not detect High and 5-x-High concentrations, whereas concentrations at two locations (NT10 and NT9) in the YSC and three sites (HL4, QH5, and QH6) in the BS exceeded the 5-x-High concentrations. Thirty-three locations [YSC (n = 10) and BS (n = 23)] exceeded ISQG guidelines, whereas five locations [YSC (n = 2) and BS (n = 3)] exceeded PEL guidelines (Table S4). Concentrations exceeding TEC were detected at one location in YSC and 12 locations in BS, whereas PEC criteria were exceeded at two locations in YSC and at one site in BS. Six locations exceeded ERL guideline and two locations exceeded ERM guidelines in YSC and BS. PAHs in the sediment of the YS and BS mostly exceeded the criteria of CCME, but did not exceed all of the criteria for locations along the YSK. Most of the sampled locations that exceeded threshold criteria were situated near industrial and municipal areas, suggesting that PAH pollution is closely associated with land-use intensity.

Concentrations of APs in the sediments of freshwater rivers feeding the YS and BS ranged from 0.5 to 160 ng g^{-1} dw (mean = 20 ng g^{-1} dw), whereas APs in seawater sediments ranged from 0.6 to 500 ng g^{-1} dw (mean = 23 ng g^{-1} dw). High concentrations of APs exceeded 5-x-High concentrations at location HL4 (500 ng g^{-1} dw) and location QH3 (160 ng g^{-1} dw), followed by locations QD1, GG1, QH4, and WH1. These locations comprised a variety of land-use, such as industrial, municipal, agriculture, and aquaculture land-uses, indicating that contamination by APs was site-specific and not associated with any one type of land-use. In addition, concentrations of APs in those locations were similar to concentrations measured by Jeon et al. (2017) at Geumgang (32–180 ng g^{-1} dw) and Wang et al. (2011) at Panjin and Yingkou (28–380 ng g^{-1} dw), indicating the continued use of APs. High and 5-x-High concentrations were lower than ISQG of CCME, and the number of locations measured with High concentrations of APs was similar in YS and BS. The three locations (15%) occurring in sediments of the YSK, eight locations (19%) in YSC, and eight locations (11%) occurring in the BS, indicating that contamination of sediments by APs is similar in the YS and BS seas.

The mean concentrations of SOs in the YS and BS were 16 ng g^{-1} dw (range 0.9–160 ng g^{-1} dw) at freshwater locations and 14 ng g^{-1} dw (range 0.7–220 ng g^{-1} dw) at seawater locations. We measured relatively high concentrations of SOs near industrial and municipal areas (locations HL4, NT10, QH6, DY5, and YC6) (Table S2) and only site HL4 (BS) and site NT10 (YSC) exceeded the 5-x-High concentrations (110 ng g^{-1} dw). This study is the first to report SOs concentrations in YSC and in BS. The concentrations were less than reported in the creeks feeding Lake Sihwa (mean = 400 ng g^{-1} dw) and Masan Bay (mean = 130 ng g^{-1} dw) in Korea and were similar to coastal areas of Gyeonggi Bay (mean = 25 ng g^{-1} dw) and the Geum River Estuary (mean = 14 ng g^{-1} dw) in Korea (Hong et al., 2016; Yoon et al., 2017; Lee et al., 2018). In general, we found that SOs contamination in YS and BS was lower than determined by previous studies, although we detected high concentrations at some locations, suggesting the need for further research in high concentration regions.

Sources of organic matter in sediments varied in Yellow and Bohai seas. In general, the $\delta^{13}C$ values for organic matter from terrestrial origin are about −27‰ to −25‰ (Schubert and Calvert, 2001; Lehmann et al., 2002), whereas $\delta^{13}C$ values from marine origins are about −22‰ to −20‰ (Peters et al., 1978; Meyers, 1994). The mean values of $\delta^{13}C$ in our study area were −24.0 ± 2.2‰ at freshwater locations and −22.0 ± 1.9‰ at marine (seawater) locations (Fig. S1), indicating a mixture of terrestrial and marine origins. These values are similar to the previous studies reported for the Yellow Sea and Korean coastal areas; Geum River (−32.6‰ to −19.4‰; Kang et al., 2019), Seomjin River (−29.1‰ to −24.6‰; Kang et al., 2019), Lake Sihwa and surrounding inland creeks (−32.2‰ to −20.4‰; Lee et al., 2017), and eastern Yellow Sea (−23.5‰ to −20.9‰; Yoon et al., 2016). Among locations of the study area, we found relatively low $\delta^{13}C$ values in sand beach (location SD) and estuarine sediments (locations DD2, QH4, QH7, BZ3, NT1, and NT5). These low $\delta^{13}C$ values may be due to

Table 1
Sediment quality guidelines (SQGs) for threshold effect concentrations (TECs: ISQG, TEC, and ERL) and probable-effect concentrations (PECs: PEL, PEC, and ERM) of contaminants. Concentrations are provided relative to 15th, 50th, and 85th percentiles for 125 sites. High concentrations were defined as the 85th percentile value of total concentration.

Compound	SQGs						This study				
	TECs			PECs			Concentration (%)			Criteria	
	ISQG	TEC	ERL	PEL	PEC	ERM	15th	50th	85th	High	5*High
Naphthalene	35	180	160	390	560	2100	7.1	11	20	20	100
2-methyl naphthalene	20	20	70	200	200	670	1.8	2.7	7.6	7.6	38
Acenaphthylene	5.9	5.9	44	130	130	640	1.8	2.9	8.6	8.6	43
Acenaphthene	6.7	6.7	16	89	89	500	2.4	6.0	23	23	120
Fluorene	21	77	19	140	540	540	1.9	3.1	13	13	65
Phenanthrene	87	200	240	540	1200	1500	1.7	4.8	20	20	100
Anthracene	47	57	85	250	850	1100	0.6	1.6	9.3	9.3	47
Fluoranthene	110	420	600	1500	2200	5100	1.8	7.5	51	51	250
Pyrene	150	200	670	1400	1500	2600	1.7	6.8	46	46	230
Benz(*a*)anthracene	75	110	260	690	1100	1600	1.1	4.8	44	44	220
Chrysene	110	170	380	850	1300	2800	1.8	9.4	82	82	410
Benzo(*a*)pyrene	89	150	430	760	1500	1600	1.9	8.9	110	110	550
Dibenzo(*a,h*)anthracene	6.2	33	63	140	140	260	2.9	12	93	93	460
Total PAHs	770	1600	4000	7100	23000	45000	14	62	630	630	3200
Alkylphenols	1000						2.8	11	27	27	140

biogeochemical process (e.g., decomposition by microbial activity) and/or hydrodynamic conditions such as freshwater and seawater mixing (Chen et al., 2005; Gao et al., 2012). In addition, relatively high δ^{13}C values were found in riverine system (locations JZ3, JZ4, DY2, DY3, WF5, QD2, LY4, and GG1), probably due to heavy algal blooms and/or agricultural runoff of organic material from C4 plants (Shi et al., 2017; Kang et al., 2019).

Sources of organic matter measured by carbon/nitrogen (C/N) ratios showed a pattern similar to δ^{13}C values. The C/N ratios of marine origin were between 4 and 12, whereas C/N ratios of terrestrial origin were above 12 (Wu et al., 2007; Szczepańska et al., 2012). C/N ratios in the present study ranged from 0.76 to 52 in freshwater locations and from 2.66 to 66 in seawater locations, indicating mixed sources of organic matter. Relatively low or high C/N ratios were found in riverine and estuarine sediments and from beach sand, which may be due to bacterial decomposition in response to superimposed effects of carbon and nitrogen influx or efflux into/from organic matter (Rice and Tenore, 1981; Thornton and McManus, 1994). Overall, the sediment stable isotopic signatures identified in the Yellow and Bohai seas would indicate a mixture of terrestrial and marine sources for the organic matters, with some regionally specific values

Concentrations of PTSs were correlated with particular physicochemical parameters of sediments (Fig. S2). PCA analysis showed that the PC2 axis explained the positive relationship between PTSs and TOC and the negative relationship between PTS and δ^{13}C, whereas the axis weakly correlated with grain size and C/N ratio. Results of regression analysis showed significant correlation between PTSs and TOC (positive: r = 0.29–0.65, $p < 0.01$), whereas PAHs and SOs were significantly correlated with δ^{13}C (negative: r = 0.18–0.26, $p < 0.05$). The correlative relationships with TOC were similar to that found in previous studies by Liu et al. (2013) and Yoon et al. (2017). Correlation of TOC with δ^{13}C indicates that PAHs and SOs are derived from terrestrial organic sources, as opposed to previously reported results identifying sources as originating in estuary (Yoon et al., 2017). However, both seawater and freshwater locations had high concentrations of PTSs, suggesting that the concentrations of PTS are related to the TOC and source of organic carbon, regardless of whether they are derived from coastal or more landward locations.

3.2. Assessment of potential ecological risks

We assessed the potential ecological risk posed by the detected PTSs using ISQG and PEL suggested by CCME (CCME, 2001, 2002). Of the 125 locations we sampled, concentrations of PAHs exceeded ISQG and PEL at 43 locations (Fig. 2b and Table S5). Concentrations of PAHs in sediments exceeded thresholds at 22% of seawater locations (18 of 83 locations) and 48% of freshwater locations (20 of 42 locations). Six PAHs (Na, 2-Na, BaA, Chr, BaP, and DbahA) exceeded ISQG at seawater sites DD, DL, and QD in the YSC and at sites YK, JZ, HL, QH, and TS in the BS. In freshwater locations, 10 PAHs (Na, 2-Na, Ace, Phe, Fl, Py, BaA, Chr, BaP, and DbahA) exceeded ISQG at sites DD and YC in the YSC and at sites DL, YK, PJ, JZ, HL, QH, TS, and DY in the BS. Some PAHs (including Ace, Flu, Phe, Ant, Fl, Py, BaA, Chr, BaP, and DbahA) exceeded PEL thresholds at locations NT10, NT9, HL4, QH5, and QH6. Locations in the YSK did not exceed ISQG and PEL, indicating higher potential risk to aquatic organisms in sediment of China than Korea. Most locations exceeding sediment quality guidelines were from industrial or municipal areas, indicating that land-use type affects the distributions of PAHs at concentrations that may detrimentally impact aquatic ecosystems.

Concentrations of APs-TEQ were generally lower than ISQG in both seawater and freshwater locations. We found relatively high concentrations of APs-TEQ in seawater locations in the YSC (sites YT and QD) and the freshwater area of the YSK (location GG1) and the BS (sites DY). However, in all regions, concentrations did not exceed ISQG, indicating a lower potential ecological risk of APs in the YS and BS. Overall, high potential risks to aquatic organisms were found from PAHs from sediments from YS and BS, suggesting that continuous monitoring and management would be needed.

3.3. Compositions and sources of PTSs

We confirmed the gradient in the compositions of PTSs by concentration (Fig. S3). The composition of high molecular weight (HMW: 4–6 rings) PAHs dominated the top 20% of PAHs concentration, whereas the composition of low molecular weight (LMW: 2–3 rings) PAHs increased as concentrations of PAHs declined. LMW PAHs were dominant in sediments of the YSK, but HMW PAHs dominated sediments of the YSC and BS, indicating that PAHs in those areas are derived from different sources. Among APs, the compositions of NPs and NPEOs were higher than OP and OPEOs in the top 20% of concentration of APs, with NPs being the most prevalent. At less contaminated locations, compositions of OPEOs were higher when concentrations of NPs and NPEOs were lower, which suggests that the use of NPEOs has

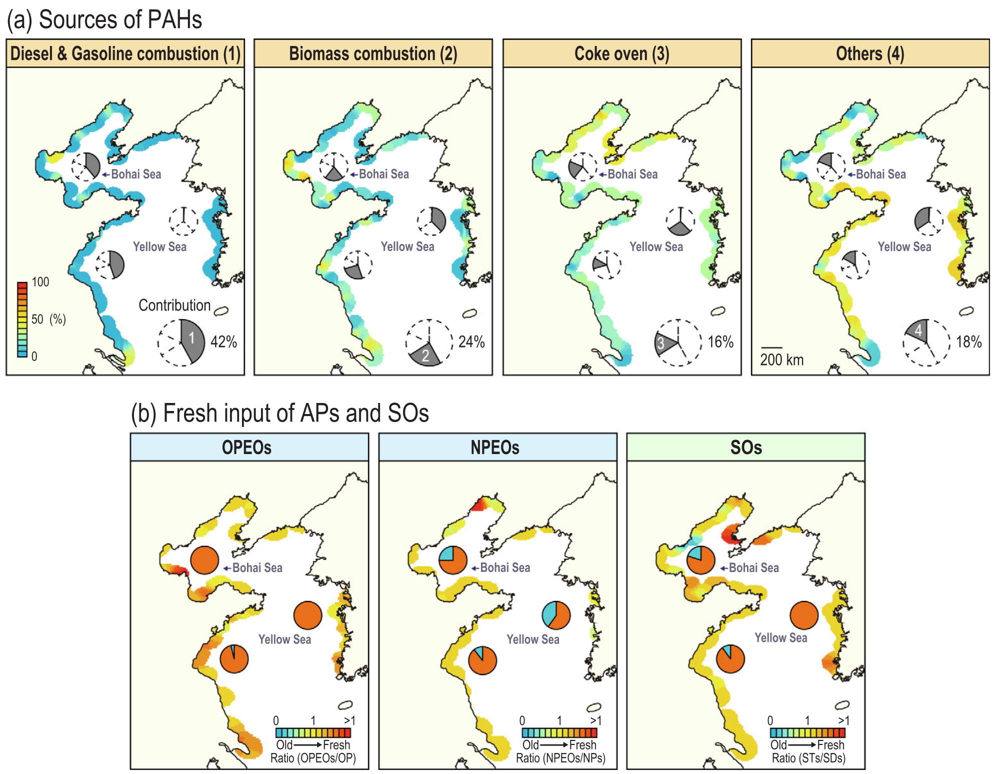

Fig. 3. Spatial-distribution of PTSs in sediments of the study area. Panels: (a) sources of PAHs derived with a PMF receptor model and (b) fresh (recent) input ratios of OPEOs, NPEOs, and SOs. The contributions represent the proportions of PTS from each source to total PTSs and regional concentrations of PAHs (Yellow Sea of Korea, Yellow Sea of China, and Bohai Sea). (For interpretation of the references to color in this figure legend, the reader is referred to the web version of this article.)

continued in highly contaminated locations. Compositions of NPEOs were highest in BS, followed by YSC and YSK, indicating that sediments in China are more contaminated by APs than Korea. Styrene trimers (STs) dominated the top 20% concentrations of SOs and the compositions of styrene dimers (SDs) increased as the concentration of SOs declined. However, the compositions of SOs in the YSK, YSC, and BS were similar, indicating that concentrations and sources of SOs are not related to specific regions, but are site-specific.

The four leading potential sources of PAHs were identified by PMF model (Fig. 3). The primary PAHs source was characterized by BbF (68%), BaP (66%), IcdP (66%), BkF (65%), BghiP (65%), Chr (60%), BaA (59%), and DbahA (55%) (Table S7). These contributors indicate that the primary source of PAHs was strongly linked to diesel and gasoline combustion (Harrison et al., 1996; Simcik et al., 1999; Ravindra et al., 2008). Diesel and gasoline sources contributed to 0.7% (YSK), 45% (YSC), and 39% (BS), for concentrations of PAHs, by region, and 42% (62000 ng g^{-1}) of the total concentration of PAHs in YS and BS. However, among all locations sampled, only nine locations were dominated by PAH from diesel and gasoline combustion. In the YSK, this source of combustion was not dominant in sediments overall, but they did dominate in three locations (NT9, NT10, and QD1) in the YSC and six locations (HL4, QH3, QH5, QH6, TS2, and TS3) in the BS. These results indicate that sources of PAHs in diesel and gasoline combustion mainly affected high concentration areas.

The secondary source of PAHs was characterized by Fl, Py, Phe, Flu, BaA, and Ant (Table S7), particularly high proportions of Fl (46%), Py (46%), and Phe (41%), which suggests that biomass combustion in the main secondary source of PAHs (McGrath et al., 2001; Guzzella et al., 2016). This secondary source of PAH contributed 35000 ng g^{-1} (24% of total PAHs) in YS and BS and 37% regionally (mainly at sites LS and GG) in the YSK, 26% (mainly at sites YC and NT) in the YSC, and 22% (mainly at sites TJ) in the BS. These results indicate that by-products of biomass combustion are more concentrated in sediments of the YSK than the YSC and BS.

The tertiary source of PAHs was dominated by Flu, DbahA, Phe, and Ant (Table S7). The major constituent, Flu (43%), is a by-product of producing coke (Kwon and Choi, 2014). In addition, major mass fractions of Phe and Ant are considered particular indicators of Coke oven combustion (Khalili et al., 1995). The signature of coke ovens mainly dominated sediments of the BS, but the regional contribution was 21%. The regional contributions of YSK and YSC were 28% and 13%, but the coke oven sources had the lowest total contribution (16%) of the total concentration of PAHs (23000 ng g^{-1}). This result indicates that coke oven by-products have the least impact in sediments of the YS and BS.

Finally, the fourth source contributor to PAH pollution in sediments was comprised of Flu, Ant, BbF, BkF, BaP, and BghiP (Table S7), but the factor profile was too low (< 20%) and was composed of a variety of chemical species. This source of PAHs occupied the highest proportion for all regions. The contribution of PAHs to sediments was 34% (YSK), 17% (YSC), 19% (BS), and 18% (26000 ng g^{-1}: contribution to total). These contributions indicated that the relatively less polluted locations are mainly dominated by the chemical species listed above (especially in the sediments of the YSK). The diagnostic ratios of PAHs also showed similar sources as those determined by the PMF model (Fig. S4). The results indicated that PAHs in the sediment of Yellow and Bohai seas were mainly derived from petroleum combustion and biomass & coal combustion. Although the ratios did not quantitatively determine the impact of each source, we observed the same trends in the Bohai Sea, where coal and biomass combustion sources were identified as dominated inputs.

We determined fresh inputs of OPEOs, NPEOs, and SOs by calculating the proportion of degraded chemicals to fresh chemicals (Hong et al., 2016; Yoon et al., 2017). In all studied regions, fresh inputs to sediments were dominant in the YS and BS. In OPEOs, all input ratios, except at QD3, suggested fresh inputs of OPEOs. The highest input ratio was found at location DY5, upstream of the Yellow River, indicating intensive use of OPEOs around the industrial area of location DY5 (Table S2). Subsequently, the ratios for sites LS, QD, AS, NT, WF, and YT were also high, indicating that OPEOs are used in all regions near the YS and BS. The fresh input of NPEOs varied by region and locations. For example, fresh inputs were high in sediments at location HL4 (adjacent to an industrial area), indicating intensive use of NPEOs by the industry located there. In addition, fresh inputs were evident at sites DD, QH4, QD7, TJ, DY, and WF in BS, at sites YT, WH, QD, RZ, LY, YC, and NT in YSC, and at sites LS and AS in YSK. In contrast, at sites YK, PJ, QH3, and QD6 in the BS, and at sites GG in YSK showed ratios exhibiting a predominance of degraded (old) NPEOs. These results indicate that recent inputs dominate most regions, but the degree of intensity is site-specific (Yoon et al., 2017).

Fresh inputs of SOs also dominated sediments in the YS and BS. At sites DL in the BS, highest fresh inputs were found in regions where we detected SDs and STs, indicating the copious use of precursors of SOs in manufacturing, such as in polystyrene production. In the YS, at sites JD and YS in YSK showed the highest fresh inputs of SOs, followed by all the other locations sampled in YSK, indicating continuous, reoccurring inputs of SOs throughout YSK. We found a predominance of degraded SOs at a few sites (HL, TS, DY, YT, and YC), with TS exhibiting the highest degradation ratio in sediments, indicating less use of plastic materials in TS than in other regions. Our results indicated that fresh inputs of SOs are derived from localized industrial and municipal activities and that they show the same trend as a previous study by Hong et al. (2016). Overall, fresh inputs of PTSs dominated the YS and BS, but distributions were regionally- and site-specific.

3.4. PTSs distributions by land-use types

The distributions of PTSs by land-uses varied by chemical constituent (Fig. 4). The highest concentrations of PAHs were associated with industrial land-use, followed (in order) by municipal, agriculture, aquaculture, saltern, barren lands, and beach land-uses. The concentrations of PAHs in industrial and municipal areas differed significantly from concentrations in other land-use types ($p < 0.05$) (Table S8). At the regional scale, concentrations of PAHs in sediments of the YSK were less than in other areas, regardless of land-use type (< 200 ng g^{-1} dw), and there were no significant differences among land-use types (Table S8). In contrast, we found significant differences in sediment concentrations in the YSC and BS between industrial, municipal, and other land-use types ($p < 0.05$). Our results indicate that concentrations of PAHs are associated with land-use type, but differ among regions. In addition, differences in the concentration of PAHs were statistically significant ($p < 0.05$) among regions relative to industrial land-use (Table S9). We attribute these differences to variations in land-use intensity in industrial areas of South Korea and China and in how the various regions pre-treat discharged wastewater (Li et al., 2010; Luo et al., 2014). The same land-use designation showed a wide range of concentrations of PAHs across regions, which in some regions correlated significantly with sediment mud content, TOC, or TN (Table S10). However, such correlations could not explain the distributions of PAH concentrations in YS and BS, which might be explained by differences in the types of other contaminants delivered from the same land-use types in different areas or the various impacts of nonpoint pollutants in sediments (Stout and Graan, 2010).

Concentrations of APs were highest in industrial areas, followed (in order) by aquaculture, municipal, saltern, agriculture, barren lands, and beach land-uses, but differences were not statistically significant ($p > 0.05$) (Table S8). At the regional scale, concentrations of APs by land-use types showed a similar trend among regions. Although the ordering of concentration of APs by land-use type varied slightly among sediments in the YSK, YSC, and BS, they were not significantly different in ranking ($p > 0.05$) (Table S8). In addition, for a given land-use type, we found a significant difference in concentrations of APs only for the beach land-use type between the YSK (mean = 5.0 ng g^{-1} dw) and YSC (mean = 11 ng g^{-1} dw) ($p < 0.05$) (Table S9), but the overall concentration was less than in other land-use types. These results indicate that for all land-use types, similar concentrations of APs accumulated in sediments of the YS and BS. Concentrations of APs by land-use types in each region could be explained by differences in environmental conditions for some regions, but we found no obvious trend in YS and BS

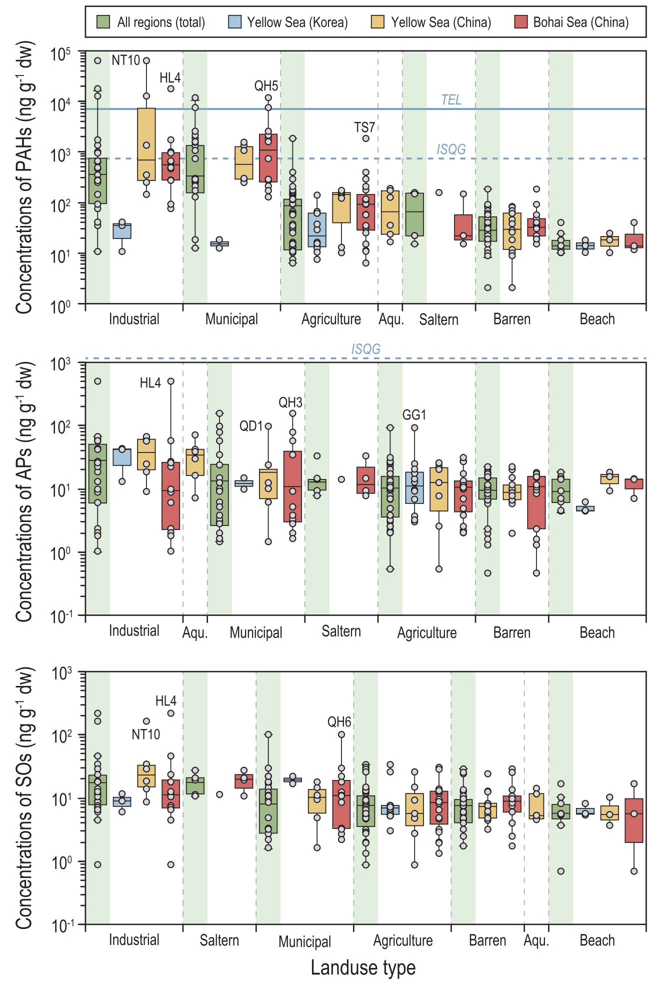

Fig. 4. Box plot of PAHs, APs, and SOs relative to seven land-use types [industrial, municipal, agriculture, beach, saltern, barren, and aquaculture (Aqu.)]. Each dot represents raw data of PTS measurements. Dotted and solid lines indicate existing sediment quality guidelines [(ISQG: interim sediment quality guidelines, PEL: probable effect levels (CCME, 2001, 2002)]

(Table S10). These results suggested that the distribution of APs is more dependent on specific pollutant sources than on land-use type or other environmental factors throughout the YS and BS, as has been found in other studies of coastal contaminants (EPA, 2010).

Concentrations of SOs in sediments associated with each land-use type differed significantly ($p < 0.05$) among types, but the post-hoc test did not identify any differences between each land-use type (Table S8). Concentrations of SOs in each region were similar regardless of land-use type with no significant difference in mean concentrations of SOs relative to land-use types ($p > 0.05$) (Table S8). Moreover, concentrations from the YSK, YSC, and BS in relative to any given land-use type were also not statistically significant ($p > 0.05$) (Table S9). Correlations of land-use type with environmental variables were region-specific (Table S10), indicating that land-use type is not significantly related to concentrations of SOs. However, relatively high concentrations of SOs in sediments at locations HL4, NT10, and QH6 were related to specific ambient sources from industrial and municipal land-uses. Hong et al. (2016, 2019) suggested that the distribution of SOs released from industrial and municipal sources are similar, but that the magnitude of release is site-specific. Overall, we found that the distributions of SOs in the YS and BS depend more on regional specific sources than by land-uses or environmental variables.

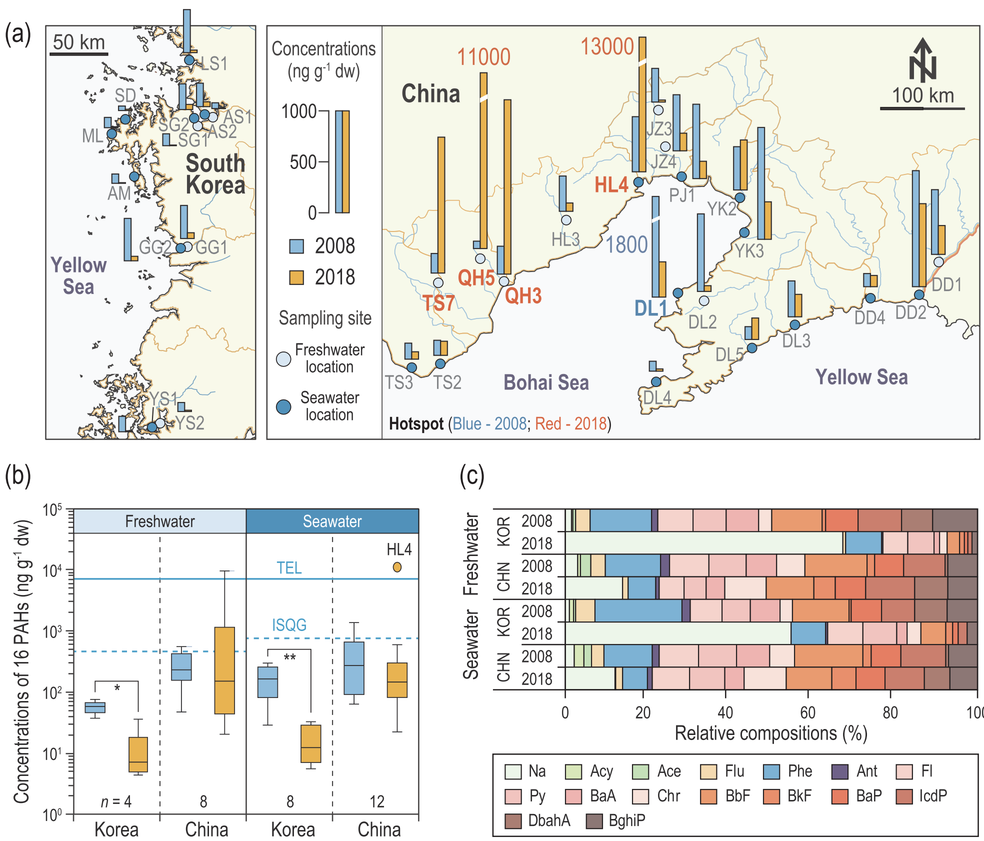

Fig. 5. The change observed over time (2008–2018) for 16 polycyclic aromatic hydrocarbons (PAHs) in sediments in South Korea and China relative to freshwater and saltwater environments. Panels: (a) spatial distribution of PAHs, (b) box plots for PAHs in freshwater and seawater locations, and (c) change in relative compositions of PAHs, by chemical species, over time. The ISQG and PEL are depicted with horizontal lines in Panel b (CCME, 2001).

3.5. Comparison of PTSs contaminations between 2008 and 2018

Change over time in the distributions of PAHs between 2008 and 2018 in Korea (YSK) and China (BS and YSC) differed (Fig. 5a). Concentrations of PAHs in YSK declined at all freshwater and seawater locations, and all locations not already exceeding sediment quality guidelines (ISQG and PEL). There was a significant difference in PAH concentrations over time at freshwater ($p < 0.05$) and at seawater locations ($p < 0.01$) (Fig. 5b). The change might be explained as a response to regulations by the Ministry of Environment (MOE, 2009) to control the release of PTSs to the environments.

In contrast, concentrations of PAHs in sediments in BS and YSC were site-specific relative to freshwater and seawater locations. Concentrations of PAHs generally declined in 2018 relative to 2008. For example, concentrations had exceeded ISQG in 2008 (1700 ng g^{-1} dw) at location DL1, but had declined 350 ng g^{-1} dw below than ISQG by 2018. However, some concentrations were many times higher in 2018 than 2008, particularly at locations TS7 (6.9 times higher), QH3 (6.2 times higher), HL4 (24 times higher), and QH5 (150 times higher), all of which exceeded ISQG and PEL guidelines. In contrast, mean concentrations of PAHs slightly declined from 2008 to 2018, but not in a statistically significant degree ($p > 0.05$). Our results indicate that environmental regulations on persistent organic pollutants have not been enforced in BS and YSC, because concentrations of PAHs have increased over the past 10 years at some locations. In addition, changes in specific sources of PAHs could explain changes in distributions of PAHs in YSK, BS, and YSC over time (2008 to 2018).

The compositions of PAHs in Korea (YSK) and China (BS and YSC) between 2008 and 2018 appear to have changed (Fig. 5c). In 2008, The HMW PAHs dominated in both freshwater (78%) and saltwater locations (70%) in YSK, whereas LMW PAHs were detected in high proportions in 2018 at both freshwater locations (77%) and seawater locations (64%). This change in predominant types of PAHs indicates that the sources in 2008 were mainly pyrogenic in origin (Gschwend and Hites, 1981; Budzinski et al., 1997). However, because LMW compounds have relatively high volatility, we speculate that sources of PAHs in 2018 were likely derived from air-water exchanges and atmospheric deposition (Tobiszewski and Namiesnik, 2012). Compositions of PAHs in BS and YSC did not change much between 2008 and 2018 at either freshwater or saltwater locations.

HMW PAHs dominated (upper 75%), regardless of year and salinity of sampling locations, but in some sites in BS, HMW PAHs concentrations increased by $> 90\%$ by 2018, such as at locations TS7, QH3, QH5, and HL4. PAHs with 5–6 rings, including BbF, BaP, IcdP, and BghiP, dramatically increased, indicating an input of diesel and gasoline combustion (Fig. S5) (Simcik et al., 1999; Ravindra et al., 2008) over the intervening 10-y period. Overall, in South Korea, concentrations of PAHs in sediments are now lower than they were 10 years prior due to efforts by the federal government to reduce PTSs. Meanwhile, higher concentrations were detected in 2018 in China, due to the lack of regulations to combat PAHs pollution. Because concentrations of PTSs were high enough to detrimentally impact aquatic ecosystems, further studies are necessary to better understand the sources, fates, and potential risks to the aquatic ecosystem.

4. Conclusions

Our study quantifies contamination by various PTSs in freshwater and seawater sediments of the Yellow and Bohai seas and describes changes that have occurred over a decadal period. We found hotspots of contamination in some rivers and coasts in China, where extremely high concentrations of PAHs pose high risks to aquatic ecosystems. Our present study shows that by-products of diesel and gasoline combustion and industrial and municipal activities contribute to more than half the PAHs contamination of sediments in the Yellow and Bohai seas. In addition, we identified fresh inputs into the Yellow and Bohai seas in both South Korea and China due to the continued use of PTSs. However, there has been a significant decline in the concentration of PAHs in

South Korea from 2008 to 2018, whereas concentrations have increased in sediment of some regions in China due to the lack of enforcement of environmental regulations. In general, contamination by PTSs in sediments of the Yellow and Bohai seas has declined since 2008, but contamination has become more severe in some specific, highly industrializing and municipalizing areas in China. Consequently, the results of the present study suggest hotspot and potential sources of contaminants, which will provide valuable information for implementing pollution reduction policies (e.g., dredging of polluted sediments, total pollution loads management, etc.) which would contribute to the improvement of sediment quality in the Yellow and Bohai seas. Stepwise monitoring and continuing management practices are needed to control contamination and potential ecological risks to the Yellow and Bohai seas marine ecosystems.

CRediT authorship contribution statement

Seo Joon Yoon: Conceptualization, Investigation, Formal analysis, Visualization, Writing - original draft, Writing - review & editing. **Seongjin Hong:** Conceptualization, Formal analysis, Resources, Writing - review & editing. **Seonju Kim:** Formal analysis, Investigation, Data curation. **Jongmin Lee:** Investigation, Formal analysis. **Taewoo Kim:** Investigation, Formal analysis. **Beomgi Kim:** Investigation, Formal analysis. **Bong-Oh Kwon:** Investigation, Project administration, Resources. **Yunqiao Zhou:** Investigation, Formal analysis. **Bin Shi:** Investigation, Formal analysis. **Peng Liu:** Investigation, Formal analysis. **Wenyou Hu:** Visualization, Project administration, Data curation. **Biao Huang:** Investigation, Project administration. **Tieyu Wang:** Conceptualization, Writing - review & editing, Project administration, Funding acquisition, Supervision. **Jong Seong Khim:** Conceptualization, Writing - review & editing, Project administration, Funding acquisition, Supervision.

Declaration of Competing Interest

The authors declare that they have no known competing financial interests or personal relationships that could have appeared to influence the work reported in this paper.

Acknowledgments

This work was supported by National Research Foundation of Korea (NRF) grants funded by the South Korean government [grant number NRF-2017R1E1A1A01075067], and also was supported by projects entitled "Integrated Management of Marine Environment and Ecosystems Around Saemangeum [grant number 20140257]", "Development of Blue Carbon Information System and Its Assessment for Management [grant number 20170318]", and "Marine Ecosystem-Based Analysis and Decision-Making Support System Development for Marine Spatial Planning [grant number 20170325]", funded by the Ministry of Oceans and Fisheries of Korea (MOF), South Korea granted to J.S.K. This work was partly supported by the National Natural Science Foundation of China (Grant No. 41877512 and 41877905), and the National Key Research and Development Project of China (2017YFC0505702). We would also like to acknowledge support from the Youth Innovation Promotion Association of the Chinese Academy of Sciences.

Appendix A. Supplementary data

Supplementary data to this article can be found online at https://doi.org/10.1016/j.envint.2020.105517.

References

Budzinski, H., Jones, I., Bellocq, J., Pierard, C., Garrigues, P., 1997. Evaluation of sediment contamination by polycyclic aromatic hydrocarbons in the Gironde estuary. Mar. Chem. 58, 85–97. https://doi.org/10.1016/S0304-4203(97)00028-5.

CCME, 2001. Canadian sediment quality guidelines for the protection of aquatic life summary tables. Updated. In: Canadian environmental quality guidelines, 1999, Canadian Council of Ministers of the Environment Winnipeg. https://www.elaw.org/system/files/sediment_summary_table.pdf.

CCME, 2002. Canadian sediment quality guidelines for the protection of aquatic life: Nonylphenol and its ethoxylates. In: Canadian environmental quality guidelines, 1999, Canadian Council of Ministers of the Environment, Winnipeg. http://ceqg-rcqe.ccme.ca/download/en/242?redir=1569847235.

Chen, B.-S., Yen, J.-H., 2013. Effect of endocrine disruptor nonylphenol on physiologic features and proteome during growth in Arabidopsis thaliana. Chemosphere 91, 468–474. https://doi.org/10.1016/j.chemosphere.2012.11.072.

Chen, C.-T.A., 2009. Chemical and physical fronts in the Bohai, Yellow and East China seas. J. Mar. Syst. 78, 394–410. https://doi.org/10.1016/j.jmarsys.2008.11.016.

Chen, J., Wang, F., Meybeck, M., He, D., Xia, X., Zhang, L., 2005. Spatial and temporal analysis of water chemistry records (1958–2000) in the Huanghe (Yellow River) basin. Global biogeochemical cycles 19. https://doi.org/10.1029/2004GB002325.

Daskalakis, K.D., O'Connor, T.P., 1995. Distribution of chemical concentrations in US coastal and estuaine sediment. Mar. Environ. Res. 40, 381–398. https://doi.org/10.1016/0141-1136(94)00150-N.

Engraff, M., Solere, C., Smith, K.E.C., Mayer, P., Dahllöf, I., 2011. Aquatic toxicity of PAHs and PAH mixtures at saturation to benthic amphipods: linking toxic effects to chemical activity. Aquat. Toxicol. 102, 142–149. https://doi.org/10.1016/j.aquatox.2011.01.009.

EPA, U.S., 2010. Nonylphenol (NP) and Nonylphenol Ethoxylates (NPEs) Action Plan. United States Environmental Protection Agency, Washington, D.C. https://www.epa.gov/sites/production/files/2015-09/documents/rin2070-za09_np-npes_action_plan_final_2010-08-09.pdf.

Gao, X., Yang, Y., Wang, C., 2012. Geochemistry of organic carbon and nitrogen in surface sediments of coastal Bohai Bay inferred from their ratios and stable isotopic signatures. Mar. Pollut. Bull. 64, 1148–1155. https://doi.org/10.1016/j.marpolbul.2012.03.028.

Ghosh, P., Gupta, A., Thakur, I.S., 2015. Combined chemical and toxicological evaluation of leachate from municipal solid waste landfill sites of Delhi. India. Environ. Sci. Pollut. Res. 22, 9148–9158. https://doi.org/10.1007/s11356-015-4077-7.

Giesy, J.P., Snyder, E.M., 1998. Xenobiotic modulation of endocrine function in fishes. In: Kendall, R., Dickerson, R., Giesy, J.P., Suk, W. (Eds.), Principles and Processes for Evaluating Endocrine Disruption in Wildlife. SETAC Press, Pensacola, pp. 155–237. https://doi.org/10.1002/etc.5620150801.

Gschwend, P.M., Hites, R.A., 1981. Fluxes of polycyclic aromatic hydrocarbons to marine and lacustrine sediments in the northeastern United States. Geochim. Cosmochim. Ac. 45, 2359–2367. https://doi.org/10.1016/0016-7037(81)90089-2.

Guzzella, L., Salerno, F., Freppaz, M., Roscioli, C., Pisanello, F., Poma, G., 2016. POP and PAH contamination in the southern slopes of Mt. Everest (Himalaya, Nepal): long-range atmospheric transport, glacier shrinkage, or local impact of tourism? Sci. Total Environ. 544, 382–390. https://doi.org/10.1016/j.scitotenv.2015.11.118.

Harrison, R.M., Smith, D., Luhana, L., 1996. Source apportionment of atmospheric polycyclic aromatic hydrocarbons collected from an urban location in Birmingham, UK. Environ. Sci. Technol. 30, 825–832. https://doi.org/10.1021/es950252d.

Hoagland, P., Jin, D., 2006. Accounting for Economic Activities on Large Marine Ecosystems and Regional Seas. NOAA's Large Marine Ecosystems (LMEs) and UNEP Regional Seas Programme. https://wedocs.unep.org/bitstream/handle/20.500.11822/11814/rsrs181.pdf?sequence=1&amp%3BisAllowed=.

Hong, S., Lee, Y., Yoon, S.J., Lee, J., Kang, S., Won, E.-J., Hur, J., Khim, J.S., Shin, K.-H., 2019. Carbon and nitrogen stable isotope signatures linked to anthropogenic toxic substances pollution in a highly industrialized area of South Korea. Mar. Pollut. Bull. 144, 152–159. https://doi.org/10.1016/j.marpolbul.2019.05.006.

Hong, S., Lee, J., Lee, C., Yoon, S.J., Jeon, S., Kwon, B.-O., Lee, J.-H., Giesy, J.P., Khim, J.S., 2016. Are styrene oligomers in coastal sediments of an industrial area aryl hydrocarbon-receptor agonists? Environ. Pollut. 213, 913–921. https://doi.org/10.1016/j.envpol.2016.03.025.

Hong, S., Khim, J.S., Ryu, J., Park, J., Song, S.J., Kwon, B.-O., Choi, K., Ji, K., Seo, J., Lee, S., 2012a. Two years after the *Hebei Spirit* oil spill: residual crude-derived hydrocarbons and potential AhR-mediated activities in coastal sediments. Environ. Sci. Technol. 46, 1406–1414. https://doi.org/10.1021/es203491b.

Hong, S., Khim, J.S., Naile, J.E., Park, J., Kwon, B.-O., Wang, T., Lu, Y., Shim, W.J., Jones, P.D., Giesy, J.P., 2012b. AhR-mediated potency of sediments and soils in estuarine and coastal areas of the Yellow Sea region: a comparison between Korea and China. Environ. Pollut. 171, 216–225. https://doi.org/10.1016/j.envpol.2012.08.001.

Jeon, S., Hong, S., Kwon, B.-O., Park, J., Song, S.J., Giesy, J.P., Khim, J.S., 2017. Assessment of potential biological activities and distributions of endocrine-disrupting chemicals in sediments of the west coast of South Korea. Chemosphere 168, 441–449. https://doi.org/10.1016/j.chemosphere.2016.10.089.

Jiao, W., Wang, T., Khim, J.S., Luo, W., Hu, W., Naile, J.E., Giesy, J.P., Lu, Y., 2012. PAHs in surface sediments from coastal and estuarine areas of the northern Bohai and Yellow Seas, China. Environ. Geochem. Health 34, 445–456. https://doi.org/10.1007/s10653-011-9445-8.

Kang, S., Kim, J.-H., Kim, D., Song, H., Ryu, J.-S., Ock, G., Shin, K.-H., 2019. Temporal variation in riverine organic carbon concentrations and fluxes in two contrasting estuary systems: Geum and Seomjin, South Korea. Environ. Int. 133, 105126. https://doi.org/10.1016/j.envint.2019.105126.

Karstens, S., Buczko, U., Jurasinski, G., Peticzka, R., Glatzel, S., 2016. Impact of adjacent land use on coastal wetland sediments. Sci. Total Environ. 550, 337–348. https://doi.org/10.1016/j.scitotenv.2016.01.079.

Khalili, N.R., Scheff, P.A., Holsen, T.M., 1995. PAH source fingerprints for coke ovens,

diesel and gasoline engines, highway tunnels, and wood combustion emissions. Atmos. Environ. 29, 533–542. https://doi.org/10.1016/1352-2310(94)00275-P.
Khim, J.S., Park, J., Song, S.J., Yoon, S.J., Noh, J., Hong, S., Kwon, B.-O., Ryu, J., Zhang, X., Wang, T., 2018a. Chemical-, site-, and taxa-dependent benthic community health in coastal areas of the Bohai Sea and northern Yellow Sea: a sediment quality triad approach. Sci. Total Environ. 645, 743–752. https://doi.org/10.1016/j.scitotenv.2018.07.169.
Khim, J.S., Hong, S., Yoon, S.J., Nam, J., Ryu, J., Kang, S.-G., 2018b. A comparative review and analysis of tentative ecological quality objectives (EcoQOs) for protection of marine environments in Korea and China. Environ. Pollut. 242, 2027–2039. https://doi.org/10.1016/j.envpol.2018.06.094.
Khim, J.S., Villeneuve, D.L., Kannan, K., Lee, K.T., Snyder, S.A., Koh, C.H., Giesy, J.P., 1999. Alkylphenols, polycyclic aromatic hydrocarbons, and organochlorines in sediment from Lake Shihwa, Korea: instrumental and bioanalytical characterization. Environ. Toxicol. Chem. 18, 2424–2432. https://doi.org/10.1002/etc.5620181107.
Kimbrough, K.L., Dickhut, R.M., 2006. Assessment of polycyclic aromatic hydrocarbon input to urban wetlands in relation to adjacent land use. Mar. Pollut. Bull. 52, 1355–1363. https://doi.org/10.1016/j.marpolbul.2006.03.022.
KOSIS, 2018. Statistical database-Population, Households and Housing units. Korean Statistical Information Service. http://kosis.kr/eng/statisticsList/statisticsListIndex.do?menuId = M_01_01&vwcd = MT_ETITLE&parmTabId = M_01_01#SelectStatsBoxDiv.
Kwon, B.G., Koizumi, K., Chung, S.-Y., Kodera, Y., Kim, J.-O., Saido, K., 2015. Global styrene oligomers monitoring as new chemical contamination from polystyrene plastic marine pollution. J. Hazard. Mater. 300, 359–367. https://doi.org/10.1016/j.jhazmat.2015.07.039.
Kwon, B.G., Saido, K., Koizumi, K., Sato, H., Ogawa, N., Chung, S.-Y., Kusui, T., Kodera, Y., Kogure, K., 2014. Regional distribution of styrene analogues generated from polystyrene degradation along the coastlines of the North-East Pacific Ocean and Hawaii. Environ. Pollut. 188, 45–49. https://doi.org/10.1016/j.envpol.2014.01.019.
Kwon, H.-O., Choi, S.-D., 2014. Polycyclic aromatic hydrocarbons (PAHs) in soils from a multi-industrial city. South Korea. Sci. Total Environ. 470, 1494–1501. https://doi.org/10.1016/j.scitotenv.2013.08.031.
Larsen, R.K., Baker, J.E., 2003. Source apportionment of polycyclic aromatic hydrocarbons in the urban atmosphere: a comparison of three methods. Environ. Sci. Technol. 37, 1873–1881. https://doi.org/10.1021/es0206184.
Lee, J., Hong, S., Kwon, B.-O., Cha, S.A., Jeong, H.-D., Chang, W.K., Ryu, J., Giesy, J.P., Khim, J.S., 2018. Integrated assessment of persistent toxic substances in sediments from Masan Bay, South Korea: comparison between 1998 and 2014. Environ. Pollut. 238, 317–325. https://doi.org/10.1016/j.envpol.2018.02.064.
Lee, J., Hong, S., Yoon, S.J., Kwon, B.-O., Ryu, J., Giesy, J.P., Allam, A.A., Al-Khedhairy, A.A., Khim, J.S., 2017a. Long-term changes in distributions of dioxin-like and estrogenic compounds in sediments of Lake Sihwa, Korea: revisited mass balance. Chemosphere 181, 767–777. https://doi.org/10.1016/j.chemosphere.2017.04.074.
Lee, Y., Hong, S., Kim, M.-S., Kim, D., Choi, B.-H., Hur, J., Khim, J.S., Shin, K.-H., 2017b. Identification of sources and seasonal variability of organic matter in Lake Sihwa and surrounding inland creeks, South Korea. Chemosphere 177, 109–119. https://doi.org/10.1016/j.chemosphere.2017.02.148.
Lehmann, M.F., Bernasconi, S.M., Barbieri, A., McKenzie, J.A., 2002. Preservation of organic matter and alteration of its carbon and nitrogen isotope composition during simulated and in situ early sedimentary diagenesis. Geochim. Cosmochim. Ac 66, 3573–3584. https://doi.org/10.1016/S0016-7037(02)00968-7.
Li, Y., Duan, X., Li, X., Zhang, D., 2013. Photodegradation of nonylphenol by simulated sunlight. Mar. Pollut. Bull. 66, 47–52. https://doi.org/10.1016/j.marpolbul.2012.11.014.
Li, Y., Zhu, X., Sun, X., Wang, F., 2010. Landscape effects of environmental impact on bay-area wetlands under rapid urban expansion and development policy: a case study of Lianyungang, China. Landsc. Urban Plan. 94, 218–227. https://doi.org/10.1016/j.landurbplan.2009.10.006.
Lin, D., Zhu, L., 2004. Polycyclic aromatic hydrocarbons: pollution and source analysis of a black tea. J. Agric. Food Chem. 52, 8268–8271. https://doi.org/10.1021/jf048636n.
Liu, A., Duodu, G.O., Mummullage, S., Ayoko, G.A., Goonetilleke, A., 2017. Hierarchy of factors which influence polycyclic aromatic hydrocarbons (PAHs) distribution in river sediments. Envrion. Pollut. 223, 81–89. https://doi.org/10.1016/j.envpol.2016.12.034.
Liu, Y., Beckingham, B., Ruegner, H., Li, Z., Ma, L., Schwientek, M., Xie, H., Zhao, J., Grathwohl, P., 2013. Comparison of sedimentary PAHs in the rivers of Ammer (Germany) and Liangtan (China): differences between early-and newly-industrialized countries. Environ. Sci. Technol. 47, 701–709. https://doi.org/10.1021/es3031566.
Long, E.R., Macdonald, D.D., Smith, S.L., Calder, F.D., 1995. Incidence of adverse biological effects within ranges of chemical concentrations in marine and estuarine sediments. Environ. Manag. 19, 81–97. https://doi.org/10.1007/BF02472006.
Luo, Y., Guo, W., Ngo, H.H., Nghiem, L.D., Hai, F.I., Zhang, J., Liang, S., Wang, X.C., 2014. A review on the occurrence of micropollutants in the aquatic environment and their fate and removal during wastewater treatment. Sci. Total Environ. 473, 619–641. https://doi.org/10.1016/j.scitotenv.2013.12.065.
Ma, M., Feng, Z., Guan, C., Ma, Y., Xu, H., Li, H., 2001. DDT, PAH and PCB in sediments from the intertidal zone of the Bohai Sea and the Yellow Sea. Mar. Pollut. Bull. 42, 132–136. https://doi.org/10.1016/S0025-326X(00)00118-1.
McGrath, T., Sharma, R., Hajaligol, M., 2001. An experimental investigation into the formation of polycyclic-aromatic hydrocarbons (PAH) from pyrolysis of biomass materials. Fuel 80, 1787–1797. https://doi.org/10.1016/S0016-2361(01)00062-X.
Meng, J., Hong, S., Wang, T., Li, Q., Yoon, S.J., Lu, Y., Giesy, J.P., Khim, J.S., 2017. Traditional and new POPs in environments along the Bohai and Yellow Seas: an overview of China and South Korea. Chemosphere 169, 503–515. https://doi.org/10.1016/j.chemosphere.2016.11.108.
Meyers, P.A., 1994. Preservation of elemental and isotopic source identification of sedimentary organic matter. Chem. Geol. 114, 289–302. https://doi.org/10.1016/0009-2541(94)90059-0.
MOE, 2009. The National Implementation Plan of the Republic of Korea under the Stockholm Convention on Persistent Organic Pollutants. Ministry of Environment. https://www.informea.org/en/action-plan/national-implementation-plan-republic-korea-under-stockholm-convention-persistent.
Moon, H.-B., Kannan, K., Lee, S.-J., Ok, G., 2006. Atmospheric deposition of polycyclic aromatic hydrocarbons in an urban and a suburban area of Korea from 2002 to 2004. Arch. Environ. Contam. Toxicol. 51, 494–502. https://doi.org/10.1007/s00244-006-0002-x.
National Bureau of Statistics, 2018. New statistical yearbooks published by China statistics press, Population, Population at year-end by region. http://www.stats.gov.cn/tjsj/ndsj/2018/indexeh.htm.
NOAA, National Status and Trends Program, 1991. Second Summary of Data on chemical contaminants in sediment from the national status and trends program. National Oceanic and Atmospheric Administration. NOAA Tech. Memo. NOS ORCA (Formerly OMA) 59, NOAA Office of Oceanography and Marine Assessment, Rockville, MD. https://repository.library.noaa.gov/view/noaa/2865.
Norris, G., Duvall, R., Brown, S., Bai, S., 2014. EPA Positive Matrix Factorization (PMF) 5.0 Fundamentals and User Guide Prepared for the U.S. Environmental Protection Agency Office of Research and Development, Washington, DC, EPA/600/R-14/108 (NTIS PB2015-105147) https://cfpub.epa.gov/si/si_public_record_report.cfm?dirEntryId = 308292&Lab = NERL.
Ohyama, K., Nagai, F., Tsuchiya, Y., 2001. Certain styrene oligomers have proliferative activity on MCF-7 human breast tumor cells and binding affinity for human estrogen receptor. Environ. Health Perspect. 109, 699–703. https://doi.org/10.1289/ehp.01109699.
Peters, K., Sweeney, R., Kaplan, I., 1978. Correlation of carbon and nitrogen stable isotope ratios in sedimentary organic matter 1. Limnol. Oceanogr. 23, 598–604. https://doi.org/10.4319/lo.1978.23.4.0598.
Ravindra, K., Sokhi, R., Van Grieken, R., 2008. Atmospheric polycyclic aromatic hydrocarbons: source attribution, emission factors and regulation. Atmos. Environ. 42, 2895–2921. https://doi.org/10.1016/j.atmosenv.2007.12.010.
Rice, D.L., Tenore, K.R., 1981. Dynamics of carbon and nitrogen during the decomposition of detritus derived from estuarine macrophytes. Estuarine, Coastal and Shelf Science 13, 681–690. https://doi.org/10.1016/S0302-3524(81)80049-7.
Saxena, G., Marzinelli, E.M., Naing, N.N., He, Z.L., Liang, Y.T., Tom, L., Mitra, S., Ping, H., Joshi, U.M., Reuben, S., Mynampati, K.C., Mishra, S., Umashankar, S., Zhou, J.Z., Andersen, G.L., Kjelleberg, S., Swarup, S., 2015. Ecogenomics reveals metals and land-use pressures on microbial communities in the waterways of a megacity. Environ. Sci. Technol. 49, 1462–1471. https://doi.org/10.1021/es504531s.
Schubert, C.J., Calvert, S.E., 2001. Nitrogen and carbon isotopic composition of marine and terrestrial organic matter in Arctic Ocean sediments: implications for nutrient utilization and organic matter composition. Deep Sea Res. Part 1 Oceanogr. Res. Pap. 48, 789–810. https://doi.org/10.1016/S0967-0637(00)00069-8.
Shi, H., Wang, X., Xu, M., Zhang, H., Luo, Y., 2017. Characteristics of soil C: N ratio and δ 13 C in wheat-maize cropping system of the North China Plain and influences of the Yellow River. Scientific reports 7, 16854. https://doi.org/10.1038/s41598-017-17060-3.
Simcik, M.F., Eisenreich, S.J., Lioy, P.J., 1999. Source apportionment and source/sink relationships of PAHs in the coastal atmosphere of Chicago and Lake Michigan. Atmos. Environ. 33, 5071–5079. https://doi.org/10.1016/S1352-2310(99)00233-2.
Solberg, T., Tiefenthaler Jr, J., O'Brien, G., Behnke, H., Poulson, H., Ela, J., Willett, S., 2003. Consensus-Based Sediment Quality Guidelines. Recommendations for Use & Application Interim Guidance. Developed by the Contaminated Sediment Standing Team, Wisconsin Department of Natural Resources. https://dnr.wi.gov/files/PDF/pubs/rr/RR088.pdf.
Stout, S.A., Graan, T.P., 2010. Quantitative source apportionment of PAHs in sediments of Little Menomonee River, Wisconsin: weathered creosote versus urban background. Environ. Sci. Technol. 44, 2932–2939. https://doi.org/10.1021/es903353z.
Szczepańska, A., Zaborska, A., Maciejewska, A., Kuliński, K., Pempkowiak, J., 2012. Distribution and origin of organic matter in the Baltic Sea sediments dated with 210Pb and 137Cs. Geochronometria 39, 1–9. https://doi.org/10.2487/s13386-011-0058-x.
Tatarazako, N., Takao, Y., Kishi, K., Onikura, N., Arizono, K., Iguchi, T., 2002. Styrene dimers and trimers affect reproduction of daphnid (Ceriodaphnia dubia). Chemosphere 48, 597–601. https://doi.org/10.1016/S0045-6535(02)00119-4.
Thornton, S., McManus, J., 1994. Application of organic carbon and nitrogen stable isotope and C/N ratios as source indicators of organic matter provenance in estuarine systems: evidence from the Tay Estuary, Scotland. Estuarine, Coastal and Shelf Science 38, 219–233. https://doi.org/10.1006/ecss.1994.1015.
Tobiszewski, M., Namieśnik, J., 2012. PAH diagnostic ratios for the identification of pollution emission sources. Environ. Pollut. 162, 110–119. https://doi.org/10.1016/j.envpol.2011.10.025.
Wang, L., Ying, G.-G., Zhao, J.-L., Liu, S., Yang, B., Zhou, L.-J., Tao, R., Su, H.-C., 2011. Assessing estrogenic activity in surface water and sediment of the Liao River system in northeast China using combined chemical and biological tools. Environ. Pollut. 159, 148–156. https://doi.org/10.1016/j.envpol.2010.09.017.
Wang, R.M., Tang, J.H., Xie, Z.Y., Mi, W.Y., Chen, Y.J., Wolschke, H., Tian, C.G., Pan, X.H., Luo, Y.M., Ebinghaus, R., 2015. Occurrence and spatial distribution of organophosphate ester flame retardants and plasticizers in 40 rivers draining into the Bohai Sea, north China. Environ. Pollut. 198, 172–178. https://doi.org/10.1016/j.envpol.2014.12.037.
White, R., Jobling, S., Hoare, S., Sumpter, J., Parker, M., 1994. Environmentally

persistent alkylphenolic compounds are estrogenic. Endocrinology 135, 175–182. https://doi.org/10.1210/endo.135.1.8013351.

Wu, Y., Zhang, J., Liu, S.M., Zhang, Z.F., Yao, Q.Z., Hong, G.H., Cooper, L., 2007. Sources and distribution of carbon within the Yangtze River system. Estuar. Coast. Shelf Sci. 71, 13–25. https://doi.org/10.1016/j.ecss.2006.08.016.

Yoon, S.-H., Kim, J.-H., Yi, H.-I., Yamamoto, M., Gal, J.-K., Kang, S., Shin, K.-H., 2016. Source, composition and reactivity of sedimentary organic carbon in the river-dominated marginal seas: a study of the eastern Yellow Sea (the northwestern Pacific). Continental Shelf Research 125, 114–126. https://doi.org/10.1016/j.csr.2016.07.010.

Yoon, S.J., Hong, S., Kim, T., Lee, J., Kwon, B.-O., Allam, A.A., Al-khedhairy, A.A., Khim, J.S., 2019. Occurrence and bioaccumulation of persistent toxic substances in sediments and biota from intertidal zone of Abu Ali Island, Arabian Gulf. Mar. Pollut. Bull. 144, 243–252. https://doi.org/10.1016/j.marpolbul.2019.05.008.

Yoon, S.J., Hong, S., Kwon, B.-O., Ryu, J., Lee, C.-H., Nam, J., Khim, J.S., 2017. Distributions of persistent organic contaminants in sediments and their potential impact on macrobenthic faunal community of the Geum River estuary and Saemangeum coast, Korea. Chemosphere 173, 216–226. https://doi.org/10.1016/j.chemosphere.2017.01.031.

Zhang, T., Yang, W.-L., Chen, S.-J., Shi, D.-L., Zhao, H., Ding, Y., Huang, Y.-R., Li, N., Ren, Y., Mai, B.-X., 2014. Occurrence, sources, and ecological risks of PBDEs, PCBs, OCPs, and PAHs in surface sediments of the Yangtze River Delta city cluster. China. Environ. Monit. Assess. 186, 5285–5295. https://doi.org/10.1007/s10661-014-3777-7.

Zhen, X., Tang, J., Xie, Z., Wang, R., Huang, G., Zheng, Q., Zhang, K., Sun, Y., Tian, C., Pan, X., 2016. Polybrominated diphenyl ethers (PBDEs) and alternative brominated flame retardants (aBFRs) in sediments from four bays of the Yellow Sea, North China. Environ. Pollut. 213, 386–394. https://doi.org/10.1016/j.envpol.2016.02.042.

<Supplementary Materials>

Large-scale monitoring and ecological risk assessment of persistent toxic substances in riverine, estuarine, and coastal sediments of the Yellow and Bohai seas

Seo Joon Yoon, Seongjin Hong, Seonju Kim, Jongmin Lee, Taewoo Kim, Beomgi Kim, Bong-Oh Kwon, Yunqiao Zhou, Bin Shi, Peng Liu, Wenyou Hu, Biao Huang, Tieyu Wang*, and Jong Seong Khim*

Table of Contents

Supplementary Tables

Supplementary Figures

***Corresponding Authors.**
E-mail addresses: wangtieyu@163.com (T. Wang); jskocean@snu.ac.kr (J.S. Khim).

Supplementary Tables

Table S1. Top 20 LMEs in Marine Industry Activity Index (Hoagland and Jin, 2006).

LME	LME#	Socioeconomic Index	Fishery & Aquaculture Index	Tourism Index	Ship & Oil Index	Marine Industry Activity Index
Yellow Sea	48	73.4	71.8	44.4	36.9	45.4
East China Sea	47	84.1	51.9	30.8	42.1	41.8
East Bering Sea	1	93.9	17.4	57.9	44.0	41.4
Insular Pacific-Hawaiian	10	93.9	17.4	57.9	44.0	41.4
Northeast U.S. Continental Shelf	7	94.0	15.5	52.8	37.9	36.4
Gulf of Mexico	5	89.1	13.0	46.3	36.6	33.8
Kuroshio Current	49	93.6	18.3	6.7	45.8	32.5
California Current	3	88.0	12.1	43.7	35.0	32.2
Gulf of Alaska	2	94.0	13.7	48.2	32.5	31.9
Southeast U.S. Continental Shelf	6	90.8	13.1	44.0	33.1	31.3
Chukchi Sea	54	87.4	14.7	34.9	27.5	26.4
South China Sea	36	73.8	34.5	22.3	14.9	20.3
Beaufort Sea	55	94.2	9.2	36.5	18.6	20.3
Gulf of California	4	80.2	4.9	24.9	23.1	19.8
Norwegian Shelf	21	95.6	10.7	3.7	28.0	19.7
Sea of Japan	50	83.3	13.3	3.5	24.0	17.7
Celtic-Biscay Shelf	24	92.2	2.5	38.8	14.6	17.0
North Sea	22	94.0	5.3	14.4	16.4	13.8
Oyashio Current	51	83.3	13.0	2.1	14.9	12.0
Iberian Coastal	25	91.2	2.5	47.3	3.2	11.9

Hoagland, P., Jin, D., 2006. Accounting for Economic Activities on Large Marine Ecosystems and Regional Seas. NOAA's Large Marine Ecosystems (LMEs) and UNEP Regional Seas Programme. https://wedocs.unep.org/bitstream/handle/20.500.11822/11814/rsrs181.pdf?sequence=1&amp%3BisAllowed=

Table S2. Information on sampling stations and conditions by each team.

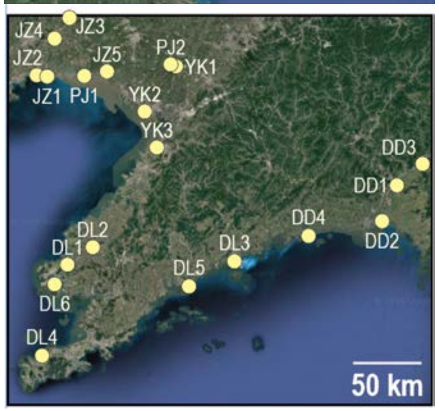

Map of sampling locations	Date (yyyymmdd)	Site	Latitude (°N)	Longitude (°E)	Land use type	Temperature (°C)	Salinity (‰)	DO (mg L^{-1})	pH
	Team 1								
	20180701	DL4	38.9844	121.5103	Beach	26.1	1.2*	9.09	7.82
	20180701	DL6	39.5058	121.4033	Unused land	26.4	35.5	8.03	7.89
	20180701	DL1	39.6208	121.5214	Industrial	25.4	34.9	7.51	7.93
	20180701	DL2	39.6947	121.740.	Industrial	27.9	0.76	9.83	8.59
	20180702	DL5	39.4817	122.5592	Municipal	24.5	34.6	7.35	7.84
	20180702	DL3	39.6633	122.9939	Municipal	26.2	31.8	6.09	7.69
	20180702	DD4	39.8383	123.6528	Agricultural	25.0	9.9*	6.62	8.36
	20180703	DD3	40.3122	124.6968	Agricultural	25.0	0.24	9.52	8.32
	20180703	DD1	40.1771	124.4567	Industrial	22.5	0.15	8.90	8.12
	20180703	DD2	39.9436	124.2828	Unused land	25.1	0.40*	5.61	7.97
	20180704	YK3	40.425	122.2844	Industrial	27.9	38.5	4.81	7.82
	20180704	YK2	40.69	122.1292	Industrial	29.1	35.3	7.20	8.30
	20180704	YK1	40.9963	122.4638	Municipal	30.4	0.64	13.8	8.84
	20180704	PJ2	41.0238	122.4338	Municipal	29.5	0.81	4.77	8.11
	20180705	JZ5	40.9092	121.8192	Industrial	29.0	36.5	7.41	7.96
	20180705	PJ1	40.8822	121.5714	Agricultural	31.8	0.50*	10.3	8.54
	20180705	JZ3	41.4531	121.4594	Unused land	27.1	0.71	8.46	8.30
	20180705	JZ4	41.1763	121.3792	Industrial	28.1	0.76	9.36	8.25
	20180706	JZ2	40.9181	121.2436	Agricultural	27.8	39.2	7.59	7.68
	20180706	JZ1	40.9242	121.1867	Agricultural	28.1	37.5	8.60	8.95
	20180706	HL4	40.7469	120.9347	Industrial	30.6	9.1	11.1	7.14
	20180706	HL5	40.5919	120.7694	Agricultural	28.3	7.5	7.44	8.94
	20180707	HL3	40.3703	120.2583	Agricultural	25.3	0.43	8.07	7.77
	20180707	HL6	40.4181	120.2992	Unused land	26.7	0.54	2.99	7.20
	20180707	HL1	40.2697	120.4622	Municipal	26.2	33.7	8.73	8.00

Table S2. (Continued)

Sampling map	Date	Site	Latitude (°N)	Longitude (°E)	Land use type	Temperature (°C)	Salinity (‰)	DO (mg L^{-1})	pH
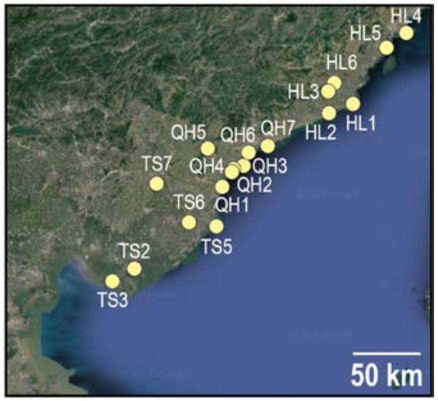	20180707	HL2	40.1747	120.2614	Agricultural	28.7	0.2	10.8	9.51
	20180708	QH7	39.9653	119.7694	Municipal	23.8	22.5	9.18	8.63
	20180708	QH6	39.9203	119.5667	Municipal	24.8	0.4*	6.28	8.47
	20180708	QH5	39.9802	119.2126	Municipal	25.8	0.4	9.88	8.81
	20180709	QH3	39.8394	119.5133	Municipal	25.0	0.5	5.36	7.23
	20180709	QH4	39.8017	119.4419	Municipal	26.2	0.3*	3.80	8.07
	20180709	QH2	39.7814	119.4136	Unused land	25.6	8.1	7.97	7.95
	20180709	QH1	39.6789	119.2911	Municipal	25.2	24.2	6.79	7.93
	20180710	TS7	39.6641	118.7881	Agricultural	26.6	0.59	5.87	0.59
	20180710	TS6	39.4607	119.1341	Agricultural	27.0	0.73	9.40	8.09
	20180710	TS5	39.4308	119.28	Agricultural	28.4	35.3	8.37	7.75
	20180710	TS2	39.1522	118.5342	Industrial	27.7	37.3	6.35	7.82
	20180710	TS3	39.0436	118.3642	Municipal	25.6	38.0	7.54	7.90
	Team 2								
	20180627	RZ1	35.298	119.4482	Aquaculture	31.3	13.8	4.9	7.7
	20180627	RZ2	35.0782	119.3033	Aquaculture	27.2	24.3	4.5	8.0
	20180628	QD4	36.2353	120.1206	Municipal	27.4	18.6	7.1	8.0
	20180628	QD5	35.8568	120.0477	Beach	27.4	21.2	13.6	8.5
	20180628	QD6	35.7684	119.9262	Aquaculture	30.1	4.4	7.1	8.1
	20180628	QD7	35.7405	119.9111	Aquaculture	29.0	14.2	3.8	7.7
	20180629	QD2	36.7802	120.4099	Unused land	29.9	0.5	16.7	10.4
	20180629	QD3	36.6637	120.295	Agricultural	30.0	0.3	12.0	9.3
	20180630	QD1	36.2609	120.3259	Municipal	31.7	18.5	3.83	7.76
	20180701	WH1	36.8266	121.4636	Aquaculture	28.7	19.9	8.0	7.9
	20180701	WH3	36.9321	121.8657	Unused land	27.6	20.9	9.8	8.3
	20180701	YT5	36.6543	120.7688	Agricultural	26.3	1.8	11.6	9.0
	20180702	WH2	37.4296	122.2754	Beach	22.4	26.9	9.2	8.2
	20180702	YT4	37.7493	120.5242	Beach	26.1	27.8	8.6	8.4
	20180702	YT6	37.5753	121.2966	Beach	25.8	28.0	9.8	8.3

Table S2. (Continued)

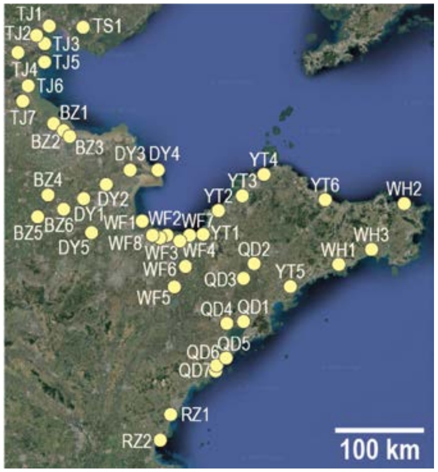

Sampling map	Date	Site	Latitude (°N)	Longitude (°E)	Land use type	Temperature (°C)	Salinity (‰)	DO (mg L^{-1})	pH
	20180703	YT1	37.1286	119.7277	Saltern	30.4	28.2	8.5	8.2
	20180703	YT2	37.4017	119.9493	Industrial	29.5	27.4	9.4	8.4
	20180703	YT3	37.5518	120.2482	Beach	29.5	17.4	9.1	8.5
	20180704	WF4	37.0765	119.4793	Unused land	28.8	25.6	7.6	8.2
	20180704	WF5	36.5802	119.3846	Agricultural	31.2	0.8	18.1	9.2
	20180704	WF6	36.7421	119.5374	Agricultural	26.1	1.7	0.3	7.4
	20180704	WF7	37.0921	119.5599	Unused land	29.0	33.7	21.8	3.7
	20180705	WF1	37.2751	118.9848	Unused land	30.0	5.2	4.8	7.9
	20180705	WF2	37.1354	119.2870	Saltern	29.8	23.5	8.9	8.2
	20180705	WF3	37.1401	119.1434	Saltern	32.1	29.7	12.6	8.8
	20180705	WF8	37.1330	119.1860	Saltern	31.3	37.0	9.0	8.5
	20180705	DY5	38.1363	118.4322	Industrial	30.5	1.6	9.4	8.1
	20180706	DY2	37.6046	118.5384	Agricultural	30.1	0.3	7.6	8.2
	20180706	DY3	37.7481	118.8214	Agricultural	-	-	-	-
	20180706	DY4	37.7615	119.1706	Unused land	33.1	0.5	8.4	8.4
	20180707	DY1	37.4851	118.2691	Agricultural	29.3	0.5	7.4	8.5
	20180707	BZ4	37.5010	117.8540	Agricultural	32.2	0.8	16.3	8.9
	20180707	BZ5	37.2497	117.7231	Agricultural	30.5	0.4	5.1	8.2
	20180707	BZ6	37.3350	118.0576	Agricultural	29.9	0.3	7.1	8.5
	20180708	BZ1	38.2637	117.8511	Agricultural	28.0	31.6	7.3	8.3
	20180708	BZ2	38.2006	118.0047	Unused land	28.0	33.3	5.3	7.6
	20180708	BZ3	38.1460	118.0528	Unused land	27.2	15.7	8.4	8.4
	20180709	TJ1	39.2000	117.7641	Industrial	-	2.2	9.4	9.5
	20180709	TJ2	39.1640	117.6623	Unused land	26.8	0.7	10.2	9.3
	20180709	TJ3	39.0938	117.7298	Unused land	25.8	22.0	5.8	8.1
	20180709	TJ5	38.9695	117.7315	Industrial	26.4	15.7	7.7	8.4
	20180710	TJ4	39.0214	117.4955	Agricultural	27.9	6.2	10.1	9.0
	20180710	TJ6	38.7667	117.5694	Industrial	29.3	29.7	8.8	8.3
	20180710	TJ7	38.6547	117.5447	Unused land	29.1	19.8	6.4	8.2

Table S2. (Continued)

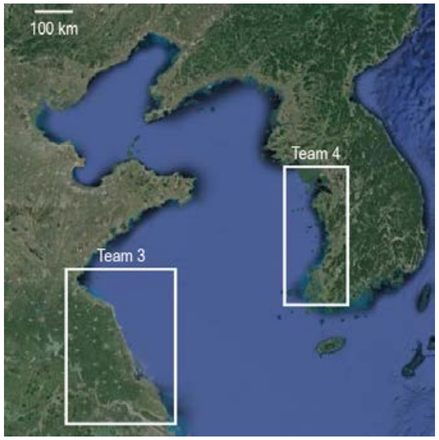

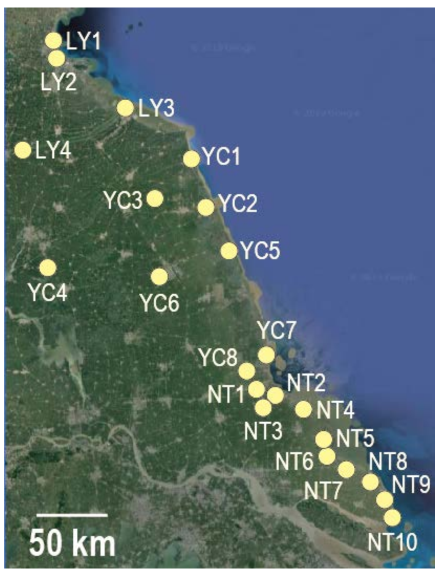

Sampling map	Date	Site	Latitude (°N)	Longitude (°E)	Land use type	Temperature (°C)	Salinity (‰)	DO (mg L^{-1})	pH
	20180710	TS1	39.0203	117.4578	Industrial	26.9	3.1	6.0	8.1
Team 3									
	20180630	LY2	34.7963	119.2244	Unused land	25.8	30.7	7.0	7.7
	20180701	LY1	34.9023	119.1961	Aquaculture	28.0	46.6	7.4	7.8
	20180701	LY3	34.5026	119.7720	Unused land	28.4	33.7	7.4	7.7
	20180701	LY4	34.1537	118.8366	Agricultural	28.0	0.5	8.1	7.9
	20180702	YC1	34.1128	120.3239	Unused land	25.4	15.0	7.2	7.8
	20180702	YC3	33.8934	120.0150	Agricultural	27.0	0.6	2.1	7.5
	20180702	YC4	33.4793	119.1460	Municipal	27.1	0.4	8.1	8.0
	20180702	YC6	33.3674	120.0770	Industrial	27.4	0.6	3.7	7.4
	20180703	YC2	33.8160	120.4768	Industrial	27.0	0.8*	2.4	7.6
	20180703	YC5	33.7400	120.5499	Unused land	28.0	20.2	7.5	7.9
	20180703	YC7	32.8821	120.9646	Unused land	28.6	41.7	5.6	7.6
	20180704	YC8	32.6933	120.8959	Unused land	28.5	4.0	9.4	8.2
	20180704	NT1	32.6031	120.9437	Industrial	29.0	2.3*	4.7	7.7
	20180704	NT2	32.5577	121.0457	Unused land	31.5	17.2	16.3	8.6
	20180704	NT3	32.5140	120.9660	Agricultural	30.0	1.4	11.7	8.2
	20180704	NT4	32.4919	121.2226	Unused land	29.4	44.6	7.9	7.9
	20180705	NT5	32.2016	121.3851	Saltern	28.8	28.1	5.1	7.4
	20180705	NT6	32.1535	121.4562	Unused land	27.7	43.1	6.7	7.7
	20180705	NT7	32.1014	121.6039	Unused land	27.5	44.6	8.2	8.1
	20180705	NT8	32.0292	121.7411	Unused land	27.0	30.8	7.5	8.0
	20180706	NT9	31.9337	121.8257	Industrial	26.7	33.3	4.3	7.6
	20180706	NT10	31.8490	121.8521	Industrial	27.4	2.0	3.1	7.7
Team 4									
	20180713	YS1	34.7821	126.4441	Municipal	28.1	26.7	7.3	8.3
	20180713	YS2	34.7866	126.4627	Municipal	29.2	0.2	5.8	9.2
	20180713	HP	35.0890	126.3538	Agricultural	34.8	31.3	4.4	7.7
	20180713	JD	34.9690	126.1662	Agricultural	25.3	32.3	7.4	8.2

Table S2. (Continued)

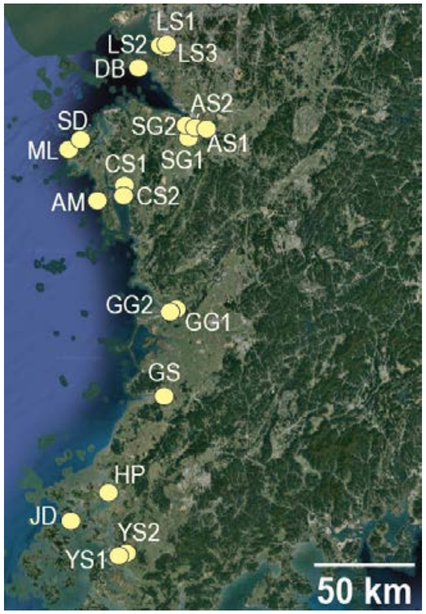

Sampling map	Date	Site	Latitude (°N)	Longitude (°E)	Land use type	Temperature (°C)	Salinity (‰)	DO (mg L^{-1})	pH
	20180714	GS	35.5728	126.6636	Agricultural	33.4	24.9	7.3	7.9
	20180714	GG1	36.0225	126.7422	Agricultural	29.3	0.1	6.7	8.7
	20180714	GG2	36.0085	126.7353	Agricultural	35.7	12.7	3.7	7.6
	20180714	AM	36.5401	126.3265	Beach	27.1	30.5	6.0	7.5
	20180714	ML	36.7838	126.1364	Beach	23.1	31.2	7.5	7.6
	20180715	SD	36.8385	126.1834	Beach	21.7	31.3	6.6	7.5
	20180715	SG1	36.8788	126.8272	Agricultural	36.6	0.2	12.0	9.7
	20180715	SG2	36.8951	126.8191	Agricultural	28.5	27.2	4.4	7.7
	20180715	AS1	36.8933	126.9123	Agricultural	32.8	0.2	10.1	9.1
	20180715	AS2	36.9154	126.9052	Agricultural	29.5	24.9	4.2	7.8
	20180716	DB	37.2142	126.5855	Agricultural	26.4	22.5	6.3	7.7
	20180716	LS1	37.3348	126.6895	Industrial	29.3	22.2	4.6	7.6
	20180716	LS2	37.3257	126.6571	Industrial	27.2	28.6	6.5	7.7
	20180716	LS4	37.3249	126.6556	Industrial	25.9	28.8	8.5	8.1
	20180723	CS1	36.5981	126.4632	Agricultural	33.3	1.5	12.7	9.3
	20180723	CS2	36.2142	126.5355	Agricultural	29.9	29.6	7.7	7.5

- Not analyzed

* The sample at these sites were collected at ebb tide time in the estuary (considered to be seawater locations).

Table S3. Instrumental conditions of gas chromatograph equipped with a mass selective detector for analyses of persistent toxic substances.

GC/MSD system	**Agilent 7890A GC and 5975C MSD**
Column	DB-5MS UI (30 m long, 0.25 mm i.d., 0.25 μm film thickness)
Gas flow	1 mL/min He
Injection mode	Splitless
Injection volume	2 μL
Injector temperature	300 °C
Ionization	EI mode (70 eV)
MS temperature	180 °C
Detector temperature	230 °C
Oven temperature (PAHs and SOs)	60 °C hold 2 min Increase 6 °C/min to 300 °C 300 °C hold 13 min
Oven temperature (APs)	60 °C hold 5 min Increase 10 °C/min to 100 °C Increase 20 °C/min to 300 °C
Targeted PAHs (39)	Naphthalene (Na), 1-Methylnaphthalene (1-Na), 2-Methylnaphthalene (2-Na), 1,3-Dimethylnaphthalene (1,3-Na), 1,4,5-Trimethylnaphthalene (1,4,5-Na), 1,2,5,6-Tetramethylnaphthalene (1,2,5,6-Na), Acenaphthylene (Acl), Acenaphthene (Ace), Fluorene (Flu), 9-Methylfluorene (9-Flu), 1-Methylfluorene (1-Flu), 1,7-Methylfluorene (1,7-Flu), 9-n-Propylfluorene (9-n-Propyl-Flu), Dibenzothiophene (Dbthio), 2-Methyldibenzothiophene (2-Dbthio), 2,4-Dimethyldibenzothiophene (2,4-Dbthio), 2,4,7-Trimethyldibenzothiophene (2,4,7-Dbthio), Phenanthrene (Phe), 3-Methylphenanthrene (3-Phe), 2-Methylphenanthrene (2-Phe), 1,6-Dimethylphenanthrene (1,6-Phe), 1,2-Dimethylphenanthrene (1,2-Phe), 1,2,9-Trimethylphenanthrene (1,2,9-Phe), 1,2,6,9-Tetramethylphenanthrene (1,2,6,9-Phe), Anthracene (Ant), Fluoranthene (Fl), Pyrene (Py), Benzo[*a*]anthracene (BaA), Chrysene (Chr), 3-Methylchrysene (3-Chr), 6-Ethylchrysene (6-Ethyl-Chr), 1,3,6-Trimethylchrysene (1,3,6-Chr), Benzo[*b*]fluoranthene (BbF), Benzo[*k*]fluoranthene (BkF), Benzo[*a*]pyrene (BaP), Perylene (Pery), Indeno[*1,2,3-c,d*]pyrene (IcdP), Dibenz[*a,h*]anthracene (DbahA), and Benzo[*g,h,i*]perylene (BghiP)
Targeted SOs (10)	1,3-Diphenylpropane (SD1), *cis*-1,2Diphenylcyclobutane (SD2), 2,4-Diphenyl-1-butene (SD3), 2,4,6-Triphenyl-1-hexene (SD4), 2,4,6-Triphenyl-1-hexene (ST1), 1e-Phenyl-4e-(1-phenylethyl)-tetralin (ST2), 1a-Phenyl-4e-(1-phenylethyl)-tetralin (ST3), 1a-Phenyl-4a-(1-phenylethyl)-tetralin (ST4), 1e-Phenyl-4a-(1-phenylethyl)-tetralin (ST5), and 1,3,5-Triphenylcyclohexane (isomer mix) (ST6)
Targeted APs (6)	4-tert-Octylphenol (OP), 4-tert-Octylphenol monoethoxylate (OP1EO), 4-tert-Octylphenol diethoxylate (OP2EO), Nonylphenols (NPs, isomer mix), Nonylphenol monoethoxylates (NP1EOs, isomer mix), and Nonylphenol diethoxylates (NP2EOs, isomer mix)

Table S4. Certified and measured concentrations for selected PAHs in standard reference material (SRM) 1944 to check the accuracy of the method.

PAHs	Certified concentration (μg g^{-1} dry weight)	Measured concentration (μg g^{-1} dry weight, $n = 3$)	Recovery (%)
Phenanthrene	5.3 ± 0.2	4.6 ± 0.3	87 ± 5.3
Fluoranthene	8.9 ± 0.3	7.8 ± 0.1	87 ± 1.6
Pyrene	9.7 ± 0.4	7.9 ± 0.3	81 ± 2.9
Benz[*a*]anthracene	4.7 ± 0.1	4.8 ± 0.2	102 ± 5.1
Chrysene	4.9 ± 0.1	4.1 ± 0.2	85 ± 3.3
Benzo[*b*]fluoranthene	3.9 ± 0.4	4.7 ± 0.2	121 ± 6.4
Benzo[*j*]fluoranthene	2.1 ± 0.4	2.1 ± 0.1	103 ± 3.6
Benzo[*k*]fluoranthene	2.3 ± 0.2	2.9 ± 0.2	126 ± 7.7
Benzo[*a*]pyrene	4.3 ± 0.1	5.3 ± 0.2	122 ± 5.1
Benzo[*e*]pyrene	3.3 ± 0.1	4.0 ± 0.1	122 ± 4.1
Perylene	1.2 ± 0.2	0.9 ± 0.1	80 ± 4.9
Indeno[1,2,3-*c*,*d*]pyrene	2.8 ± 0.1	3.3 ± 0.2	119 ± 4.9
Dibenz[*a*,*h*]anthracene	4.2 ± 0.1	5.1 ± 0.1	121 ± 1.8
Benzo[*g*,*h*,*i*]perylene	4.8 ± 0.1	3.5 ± 0.1	122 ± 2.7

Table S5. Concentrations of PAHs in sediments of the Yellow and Bohai seas.

Target PAHs	LS1	LS2	LS4	DB	AS1	AS2	SG1	SG2	SD	ML	AM	CS1	CS2	GG1	GG2	GS	HP	JD	YS1	YS2	DD1	DD2	DD3	DD4	DL3	DL5	YT5	YT6	WH1	WH2	WH3	QD1
Na	9.0	11.7	8.9	11.6	8.6	13.9	6.4	12.8	11.8	13.7	8.1	10.2	9.7	8.1	5.8	11.8	7.6	6.3	6.6	10.	35.6	33.7	16.7	17.1	19.3	17.2	6.8	9.5	16.7	13.1	16.4	22.3
2-Na	2.0	3.1	1.7	3.0	1.6	3.7	1.0	3.6	2.0	2.8	2.1	2.1	2.1	3.5	2.2	2.8	2.0	1.6	1.2	2.5	17.8	24.2	5.3	3.7	6.5	1.4	2.0	3.1	6.7	2.8	4.5	12.1
1-Na				2.1				1.2													6.0	7.6	2.1	1.4	2.3				2.2		1.3	4.0
1,3-Na																					3.4	6.4			1.5							2.8
1,4,5-Na																					1.8	6.5										2.7
1,2,5,6-Na																						4.1										2.1
Acl																																
Ace																						3.9										
Flu														1.6							3.5	12.2	2.0	2.4	4.1				2.9			6.2
9-Flu																																
1-Flu														2.2							3.7	32.5	2.0	2.9	2.1				6.9			38.1
1,7-Flu																					1.8	9.6	1.6		2.3							6.9
9-n-Propyl-Flu																																
Dbthio																																
2-Dbthio																																
2,4-Dbthio																																
2,4,7-Dbthio																																
Phe	2.6	2.7		2.4		3.3		4.2		1.3			1.3	4.4	3.6	2.2	1.6	1.6	1.6	1.9	25.7	49.4	8.9	7.3	14.2	1.8	1.2	1.9	10.2	1.8	2.7	25.3
3-Phe	0.7	0.7		0.7		0.9		1.2						1.3	1.0	0.4	0.3	0.3			3.8	15.0	1.5	1.9	4.5			0.6	5.6	0.3	0.6	17.5
2-phe	0.7	0.8		0.7		1.0		1.2						1.2	1.2					0.9	5.4	16.4	2.1	1.7	4.1				3.8			16.0
1,6-Phe	1.6	1.7		1.8		2.5		2.6						7.1	3.0	1.2	0.8	0.7			5.7	33.7	3.0	2.9	6.8			0.8	5.7			34.4
1,2-Phe																						2.3			0.7				0.9			4.7
1,2,9-Phe																																
1,2,6,9-Phe														0.9								1.2										1.5
Ant	0.4	0.4						0.7						0.7	0.5						3.0	10.6	0.8	1.1	2.3				2.3			8.0
Fl	4.2	4.0		4.3		5.4		7.5					1.2	9.1	6.5	3.0	1.8	1.5	1.5	1.2	27.6	79.3	8.1	9.3	26.1	1.5		1.7	18.1		1.3	61.1
Py	4.2	4.1		3.8		5.0		7.1					0.9	9.2	5.4	2.3	1.5	1.3	1.5	1.4	23.7	73.1	7.0	7.9	18.2	1.7		1.2	11.1			54.5
BaA	1.4	1.5		1.4		2.0		2.7						3.1	2.4	0.9	0.6				12.0	40.8	4.8	4.3	7.8	0.8		0.6	4.8			79.3
Chr	1.9	2.1		2.1		2.7		3.8						3.9	3.1	1.5					29.2	89.0	12.2	10.6	22.8	1.7		1.6	11.1		1.8	116
3-Chr	0.6	0.8		0.5		0.9		0.8						1.5	1.0						10.3	55.0	5.1	5.3	13.4	0.5		1.7	7.7			192
6-Ethyl-Chr																						2.2		0.6	0.6				0.7			8.5
1,3,6-Chr																						1.6										2.1
BbF	3.3	3.1		2.9		5.7		5.4						6.9	5.9	2.6					22.3	90.3	9.3	10.2	27.0	2.0		1.7	18.7			212
BkF						2.2		2.0						2.8	2.5						17.6	58.5	7.6	6.7	15.0	2.0			7.4			79.6
BaP						1.9		1.5						1.7	1.8						17.4	52.1	5.9	5.7	15.5	1.5			5.5			104
Pery	2.1	2.1				3.4		3.3						64.9	9.5						6.8	319	4.3	19.1	21.1	1.8			6.8			26.2
IcdP						3.0		2.0						2.6	3.0						25.4	92.5	13.2	11.5	21.0	2.7			8.0			193
DbahA																					22.1	62.7	13.1	11.0	10.8	3.2						92.9
BghiP		2.0				3.2		2.8						2.8	3.5						19.2	65.2	6.4	6.6	15.2				8.2			136

[a] Shaded concentrations indicate values that exceeded ISQG (orange) and PEL (red).

Table S5. (Continued)

Target PAHs	QD2	QD3	QD4	QD5	QD6	QD7	RZ1	RZ2	LY1	LY2	LY3	LY4	YC1	YC2	YC3	YC4	YC5	YC6	YC7	YC8	NT1	NT2	NT3	NT4	NT5	NT6	NT7	NT8	NT9	NT10	DL1	DL2
Na	14.5	28.4	17.5	7.1	8.8	8.9	10.5	8.3	6.4	7.3	2.1	8.4	7.7	8.6	6.3	13.5	5.6	18.3	5.7	5.6	9.8	5.3	9.2	11.3	13.3	13.0	16.4	12.1	19.3	128	35.0	15.2
2-Na	1.7	9.5	3.9	1.8	4.0	2.8	3.9	2.5	1.9	2.9		1.5	2.6	2.3	3.3	19.0	2.1	31.5	1.9	1.7	3.9	1.5	4.7	2.7	5.0	4.2	3.8	4.5	9.0	66.4	20.5	2.2
1-Na		3.2	1.6		1.3		1.3									6.2		11.4					1.5		1.2				2.7	32.5	9.6	
1,3-Na																5.2		12.0											2.3	16.6	6.4	
1,4,5-Na																5.9		16.4					1.7						3.2	22.3	5.1	
1,2,5,6-Na																7.6		20.0					1.7							3.7	6.3	
Acl																														8.6		
Ace																4.8		6.0											44.0	353		
Flu		4.2	2.2		2.2					1.8				2.9	2.9	8.9		14.3			1.9		1.7		2.0				149	526	4.1	2.0
9-Flu																													2.8	4.0		
1-Flu		3.5	3.0		1.7	2.0	2.4			3.5			2.3	3.9	2.0	6.5		20.3			3.0		2.0	1.8	2.6	1.8	3.0	1.6	94.5	379	2.7	2.0
1,7-Flu																1.8		4.7			1.8								5.5	14.4	1.7	
9-n-Propyl-Fl																														1.2		
Dbthio																													11.7	150		
2-Dbthio																1.2		3.8												6.9	0.9	
2,4-Dbthio																														3.9		
2,4,7-Dbthio																														1.0		
Phe	2.8	15.5	11.3	1.2	8.5	2.5	3.6	4.8	1.3	3.0			1.9	6.3	10.3	57.7	1.3	58.9		1.2	7.2	2.3	6.2	1.4	5.5	3.1	2.9	3.5	1424	5381	22.6	5.2
3-Phe	0.5	2.6	3.8		2.7	0.7	1.1	1.2	0.6	1.8			0.9	1.8	3.3	20.2	0.8	25.4	0.3	0.4	3.7	0.9	4.5		2.5	1.3	0.9	1.5	138	533	6.5	0.6
2-phe	0.7	3.5	3.6		2.4		0.9	1.1		1.0				1.1	2.0	13.2		17.0			2.1		3.1		1.6	0.9	0.7	1.1	115	968	7.9	0.7
1,6-Phe	0.7	2.9	5.5		3.1		1.2	1.3	0.9	2.5			1.1	1.7	2.6	26.8		28.3			8.8		6.7		1.7	1.7	1.3	1.4	62.5	280	11.8	
1,2-Phe			0.8													2.3		5.7											4.2	18.7	1.1	
1,2,9-Phe																														1.5		
1,2,6,9-Phe																1.1		3.6			1.7								2.6	4.9	2.1	
Ant		1.6	2.0		2.1		0.5	1.1		1.5				2.2	2.5	17.3		19.9			2.0	0.5	1.3		1.4	0.6	0.6	0.6	361	591	2.8	0.8
Fl	1.5	7.9	21.0		21.7	3.1	3.7	18.3	2.2	7.5		1.4	2.2	21.9	21.8	131		144		1.3	25.4	6.1	10.0		14.0	4.4	5.7	5.3	980	6406	24.1	2.3
Py	1.2	5.4	16.9		13.5	1.7	2.4	11.9	2.1	5.8		1.5	2.2	19.3	23.4	123		143	0.9	1.3	28.1	6.1	10.9	1.0	13.6	3.9	5.6	4.7	2619	10857	20.3	3.2
BaA	1.2	4.4	15.2		8.1		0.8	8.3	0.7	2.4			0.8	9.1	10.9	72.6		90.7			15.9	2.5	5.4		6.3	1.3	2.5	2.0	966	4152	12.8	1.6
Chr	2.8	11.7	28.3		13.7	1.3	1.7	12.6		3.0			1.3	10.0	14.0	78.4		103			19.2	3.6	7.1		8.4	2.2	3.7	3.2	1107	5072	35.0	3.6
3-Chr	2.2	16.4	27.2		9.8	0.7	1.0	3.5	0.6	1.6			0.5	2.4	5.2	24.2		42.1			8.2	0.9	3.0		2.7	0.9	1.0	1.6	214	1223	21.8	1.0
6-Ethyl-Chr		0.5	0.9		0.9									0.6	0.9	3.7		11.8			1.7		0.8		0.5				28.0	206	1.4	
1,3,6-Chr					0.7																0.6								2.8	18.2	1.5	
BbF	2.8	10.5	37.7		24.6			17.4		4.9			2.4	15.9	19.3	115		143			28.1	4.9	10.6		11.6	3.3	4.4	4.0	1189	5254	37.2	3.4
BkF		4.4	16.7		10.1			6.9		1.5				6.6	5.9	38.5		52.4			9.0		3.5		3.9		1.7		432	4652	23.9	2.4
BaP		4.3	16.8		8.8			7.0		1.4				10.6	8.1	68.1		79.0			13.2	1.8	5.1		4.9		1.9	1.8	884	4241	28.1	2.4
Pery			3.9		3.4					2.0				3.8	4.3	11.7		19.9			13.3	3.8	5.3		26.4	39.6	8.1	30.1	228	725	13.9	945
IcdP	2.7	8.3	26.4		18.2			8.3		2.2				8.2	10.9	90.7		99.1			20.2	2.5	6.4		6.2		2.0		895	7384	41.0	5.8
DbahA	2.3	6.1	15.1		2.6										2.0	17.0		19.4			3.1								165	1301	28.9	8.0
BghiP		6.7	18.7		19.3			10.2		2.1				4.7	11.3	79.4		100			17.8	2.6	8.6		6.8		2.2	1.9	790	4408	29.9	2.5

[a] Shaded concentrations indicate values that exceeded ISQG (orange) and PEL (red).

Table S5. (Continued)

Target PAHs	DL4	DL6	YK1	YK2	YK3	PJ1	PJ2	JZ1	JZ2	JZ3	JZ4	JZ5	HL1	HL2	HL3	HL4	HL5	HL6	QH1	QH2	QH3	QH4	QH5	QH6	QH7	TS1	TS2	TS3	TS5	TS6	TS7	TJ1
Na	17.2	23.6	40.0	24.4	21.8	20.7	32.8	22.5	15.8	12.5	26.8	18.4	20.4	16.1	16.1	111	16.9	10.0	16.5	11.7	19.8	27.1	12.1	36.0	14.4	9.5	16.7	14.3	10.9	15.0	19.4	10.9
2-Na	1.4	4.4	31.5	11.8	12.2	12.4	29.5	4.6	5.9	6.5	18.4	7.2	7.6	6.8	3.6	121	4.9	0.9	4.4	0.9	15.2	22.4	9.0	52.3	4.2	4.3	5.0	4.4	3.1	3.1	21.2	4.7
1-Na		1.6	8.6	3.5	4.3	6.0	9.0	1.6	2.3	3.1	8.1	2.8	2.6	2.5	1.4	45.0	1.9		1.3		6.2	8.9	3.5	17.5	1.9	1.8	2.0	1.7	1.4	1.3	7.6	
1,3-Na			5.8	2.1	3.3	4.7	6.9			1.9	4.8	2.3	1.7	1.6		51.2					5.6	7.1	1.9	13.8		1.6					6.3	
1,4,5-Na			2.1	1.7	3.0	4.8	5.8			2.0	4.4	3.6		1.8		90.4					6.1	7.7	1.7	14.4		1.8					5.1	
1,2,5,6-Na				2.0	2.3	4.4	9.6			1.7	4.3	1.9				66.7					6.0	4.9		13.8							3.1	
Acl			2.9				2.4									40.9						1.8		2.9								
Ace			15.2	3.9			14.4									23.0						2.4	15.7	7.4							2.4	
Flu		2.8	13.1	6.6	6.4	3.7	18.6	1.9	2.3		3.3	3.1	3.4	3.7	2.3	121	2.6		2.2		9.3	21.9	16.3	39.3	2.7	5.0	3.4	2.4		1.6	15.0	
9-Flu																4.8																
1-Flu		2.8	10.5	6.3	4.8	3.5	20.2	1.9	2.5	1.7	2.5	3.9		4.8	2.4	174	2.0		2.6		8.4	8.3	3.1	27.9		3.0	2.2		1.7	2.1	42.7	
1,7-Flu			2.7	2.4	4.7	2.4	6.8				2.0	3.4		1.9		170					11.3	10.9	3.3	39.8		3.8	1.9				10.4	
9-n-Propyl-Fl																3.1								1.5								
Dbthio							1.2									32.5					2.2	2.3	2.3	5.1							1.1	
2-Dbthio							1.9									29.6					2.2	1.0		3.0								
2,4-Dbthio																19.0					1.8			1.6								
2,4,7-Dbthio																22.9					2.1			1.3								
Phe	1.8	11.7	60.4	18.7	20.5	13.8	63.9	5.5	8.3	3.2	15.3	12.9	12.8	16.7	6.3	357	10.4	2.1	5.4	1.6	49.3	105	214	141	10.2	18.2	15.6	13.4	4.0	5.2	53.3	5.5
3-Phe		2.7	7.7	4.4	7.8	15.2	13.1	1.0	2.0	0.8	4.2	9.3	2.7	4.3	1.3	195	8.1	0.3	1.6		19.4	28.9	28.8	47.9	2.6	8.9	4.9	3.1	1.2	1.1	23.5	1.6
2-phe		2.7	11.5	4.9	9.3	9.5	17.3	1.4	2.4	1.1	5.6	10.4	3.4	6.6	1.8	234	5.0		1.8		22.5	36.0	37.6	68.0	3.4	8.9	5.1	3.6	1.6	1.6	23.8	1.6
1,6-Phe		4.1	11.4	10.2	14.1	18.0	38.3	2.1	4.6	2.3	10.4	28.9	4.7	12.9	4.8	715	4.1		3.9		54.0	47.9	31.3	120	6.4	34.1	8.4	7.1	1.9	2.2	43.5	2.6
1,2-Phe			1.1	0.9	1.2	1.5	2.4				1.2	1.7		0.9		68.9					5.8	4.3	2.7	12.9		3.9	1.0	0.8			3.6	
1,2,9-Phe							1.6									12.3					0.7			1.8								
1,2,6,9-Phe							1.3									38.2					2.1	1.2	1.2	5.1		4.6					1.3	
Ant		1.5	14.6	5.3	3.7	1.8	16.6	0.7	1.9	0.5	1.9	1.9	1.2	1.9	0.6	174	1.4		0.8		8.3	24.0	9.3	28.2	1.0	3.9	1.9	1.5	0.4	0.5	9.3	0.7
Fl	1.5	20.8	126	50.5	39.3	17.5	129	4.5	18.7	1.8	11.3	16.5	12.9	22.8	4.9	286	12.4		4.8		101	189	430	241	6.4	36.5	35.7	30.7	2.8	6.9	74.6	7.0
Py	1.7	16.1	107	46.1	31.1	14.2	111	4.4	14.2	1.7	11.0	14.5	10.8	19.4	4.4	916	10.0		4.8		87.3	126	345	190	5.2	27.7	25.5	23.8	2.3	5.5	49.8	6.8
BaA	0.8	8.9	86.2	32.2	18.5	7.9	96.2	2.8	9.0	1.4	8.6	8.5	6.5	13.1	2.7	742	7.8	1.1	4.6	0.7	114	189	500	390	7.0	44.3	34.5	35.5	1.8	3.7	79.5	3.6
Chr	1.7	21.5	147	57.9	45.4	25.0	173	7.2	16.0	3.4	23.2	23.5	20.1	37.4	9.4	1243	17.6	2.3	12.1	1.4	190	226	884	580	14.4	82.1	54.9	53.7	4.8	9.0	140	6.6
3-Chr	0.5	9.9	62.3	40.9	35.5	27.2	119	5.8	7.0	2.5	27.1	25.5	13.8	33.6	8.5	2857	11.1	1.4	20.4	0.6	221	237	557	843	16.4	187	40.4	46.4	3.3	6.1	314	3.8
6-Ethyl-Chr			4.9	1.5	1.3	4.5	5.0		0.6		1.2	0.9	0.7	1.5	0.5	195	0.8		0.8		14.1	8.6	24.4	45.0	1.0	5.0	2.2	2.4			8.7	
1,3,6-Chr							0.9							0.6		71.6	1.0		0.9		9.4	5.3	10.2	15.7		21.1		0.6			7.8	
BbF	2.0	25.4	212	60.7	47.2	17.0	216	4.9	16.9	2.2	15.8	19.8	20.8	42.5	8.1	1792	16.9	1.7	8.2		291	359	2138	1121	17.3	103	96.8	139	4.5	8.4	232	6.9
BkF	2.0	14.8	110	36.8	23.2	10.4	109	2.5	9.3		8.0	11.7	10.6	26.2	4.6	528	9.0	1.6	4.8		127	132	675	334	8.7	40.8	38.5	116	1.8	3.3	87.3	2.2
BaP	1.5	14.4	160	43.8	28.6	11.3	150	3.2	8.7	1.5	13.9	12.7	12.5	26.1	5.2	1631	9.1	1.5	4.8		163	179	1259	572	8.9	43.2	48.2	49.5	1.9	3.9	110	2.8
Pery	1.8	8.2	27.4	49.1	17.4	5.7	73.6		3.6		1.9	9.0	4.8	11.8	5.0	154	3.8				28.4	34.4	151	89.1	2.8	83.6	46.6	15.6			29.6	
IcdP	2.7	21.8	148	46.4	35.4	11.5	177	5.0	11.8	2.3	12.2	14.6	16.0	34.9	7.7	2124	18.1	3.7	7.1	1.9	253.	254	2382	1203	16.3	79.2	83.5	84.1	3.4	5.3	216	3.5
DbahA	3.2	12.5	68.4	25.0	21.7	8.1	77.6	5.1	6.6	2.3	12.2	8.2	8.7	18.2	4.8	1333	22.6	8.7	10.6	3.6	116	133	923	619	12.0	38.4	35.0	33.2	2.5	3.8	98.7	
BghiP		16.7	105	31.7	26.8	7.6	136	2.7	6.0		10.4	10.6	12.5	25.7	5.0	1307	10.1		4.0		177	140	1333	693	7.7	50.0	55.2	55.2	2.2	3.7	143	4.5

[a] Shaded concentrations indicate values that exceeded ISQG (orange) and PEL (red).

Table S5. (Continued)

Target PAHs	TJ2	TJ3	TJ4	TJ5	TJ6	TJ7	BZ1	BZ2	BZ3	BZ4	BZ5	BZ6	DY1	DY2	DY3	DY4	DY5	WF1	WF2	WF3	WF4	WF5	WF6	WF7	WF8	YT1	YT2	YT3	YT4
Na	12.6	11.0	10.2	7.1	10.6	7.5	6.1	6.1	6.8	9.1	8.6	7.5	10.0	11.0	4.9	6.7	20.5	10.2	10.2	11.0	6.3	8.6	9.7	11.8	12.9	8.3	11.2	8.0	8.3
2-Na	16.6	5.1	5.3	3.6	6.8	2.5	2.2	2.5	1.8	3.8	4.1	1.9	5.6	2.1	1.3	3.9	31.3	3.8	3.3	3.5	1.8	2.1	4.9	2.5	2.4	2.9	4.2	2.3	2.4
1-Na	3.3	1.3	1.4		2.0								1.9				7.3						1.7				1.4		
1,3-Na	1.8																7.0												
1,4,5-Na			1.5		1.7												7.4												
1,2,5,6-Na																	4.3												
Acl																	4.1												
Ace																	5.6												
Flu	3.3	1.8	1.7	1.9	3.1								1.9				6.4						2.3						
9-Flu																													
1-Flu	2.6		2.2	1.7	2.4								3.3				58.9	1.6		1.6			3.6				1.7		1.8
1,7-Flu																	5.6												
9-n-Propyl-Fl																													
Dbthio																	2.4												
2-Dbthio																	2.5												
2,4-Dbthio																	1.4												
2,4,7-Dbthio																													
Phe	12.3	6.1	6.1	5.8	18.5	2.5	2.1	2.1	2.0	3.9	2.8	1.3	4.8	1.4		3.1	81.7	3.6	2.3	3.6	1.7		9.5	2.0	2.2	2.1	8.9	1.2	1.2
3-Phe	4.8	2.1	4.0	2.8	6.7	1.0	0.8	0.7	0.6	1.2	0.9	0.3	2.9	0.3		1.0	36.5	1.2	0.6	2.4	0.5		2.8	0.5	0.7	0.5	2.4		
2-phe	4.0	1.8	2.8	1.8	4.8	0.8	0.7			1.3	0.9		2.2			1.2	42.2	1.0		2.0			2.4				2.5		
1,6-Phe	6.3	3.2	4.7	2.6	5.0	1.0	2.0	1.1	1.0	2.2	1.0		2.0			1.4	52.7	1.1		2.9			2.4		0.8		2.8		
1,2-Phe			0.9		1.0												5.0												
1,2,9-Phe																													
1,2,6,9-Phe			0.9														3.3												
Ant	3.0	1.0	1.4	1.6	3.2	0.4				0.7			0.8				21.9	0.8		0.6			4.4				1.5		
Fl	18.4	9.3	9.9	11.3	46.0	4.2	2.8	2.5	2.0	3.1	1.9		5.3			2.5	116	3.7	2.4	3.3	2.0		15.3	1.9	1.0	1.4	30.8		
Py	16.3	10.3	12.3	10.3	36.3	3.8	2.8	2.0	1.9	2.5	2.0		3.1			2.6	157	2.4	1.2	3.7	1.0		9.0		1.7		20.3		
BaA	8.8	4.2	5.1	4.7	15.0	1.5	1.3	0.8	0.6	1.1	0.7		1.7			1.0	125	1.2		7.2			5.3				15.9		
Chr	12.0	6.7	7.1	7.0	22.9	2.8	2.1	1.5	1.2	2.1	1.4		3.6			1.9	149	2.7	1.3	24.8	1.1		8.7				23.9		
3-Chr	4.0	3.1	6.1	3.1	7.5	1.1	1.2	0.7	0.6	1.4	0.5		1.8			0.9	97.8	3.8	0.8	44.1	0.5		3.7				10.5		
6-Ethyl-Chr		0.7	1.9	0.9	1.7												6.6	0.5		2.6			0.7				0.9		
1,3,6-Chr			0.9														1.1												
BbF	16.8	8.0	8.5	8.4	29.1	3.4	3.2	1.7		2.2			3.6			2.0	156	2.2		9.5			10.3				36.4		
BkF	5.2	2.7	2.5	2.7	9.1												59.8			3.7			3.9				16.9		
BaP	7.3	3.3	3.5	3.3	10.4												146			5.6			5.0				17.3		
Pery	5.3		2.3	2.6	2.4												18.9										4.0		
IcdP	9.5	4.5	4.3	4.1	14.3		2.0										133			2.4			4.9				27.0		
DbahA	1.8				2.9												35.1			4.7							3.3		
BghiP	10.3	5.4	5.9	4.9	15.0		2.3						1.9			2.2	135			7.2			5.6				29.3		

[a] Shaded concentrations indicate values that exceeded ISQG (orange) and PEL (red).

Table S6. Concentrations of APs and SOs in sediments of the Yellow and Bohai seas.

Sites	APs						SOs									
	OP	OP1EO	OP2EO	NP	NP1EO	NP2EO	SD1	SD2	SD3	SD4	SD5	SD6	SD7	SD8	SD9	SD10
LS1	1.28	0.97	18.17	7.44	4.23	11.90	1.33		1.95	0.30	4.32		0.47	0.58		
LS2	1.42	0.78	16.67	7.69	4.42	1.86	1.26		1.98	0.80	4.74	0.63	1.04	0.72	0.47	
LS4	0.13	0.33	6.67		1.87	4.19	1.20		1.31		3.52					
DB	0.27	0.18	5.78		9.50	4.78	1.02		1.04		2.79		0.36			
AS1		0.18	1.76		1.26		0.89		1.72		3.83		0.76			
AS2	0.12	0.23	5.69	5.21	2.11	4.22	2.20	2.20	5.88	2.68	11.64	4.45	2.35	1.46	0.85	
SG1	0.13	0.14	2.28		1.13		1.28		1.19		4.22					
SG2	0.28	0.27	6.93		2.25	4.58	1.46		1.32	0.44	3.90		0.52			
SD	0.91	0.27	2.82		1.17	1.82	1.06		1.32	0.33	3.23		0.93	1.31		
ML	0.95	0.21	2.82		1.33		1.10		1.27		2.97		0.34			
AM		0.25	2.75		1.43		1.03		1.15		2.78		0.41			
CS1	0.88	0.20	1.64		1.58		0.84				1.87		0.31			
CS2	0.13	0.27	3.16		2.93	2.73	0.89		1.09		3.12		0.49			
GG1	2.33	0.68	3.65	65.24	13.25	7.22	1.18		1.09	0.37	4.10		0.45			
GG2	0.29	0.34	1.14	4.49	3.42	6.12	1.00		1.21		3.42		0.86	0.68	0.43	
GS	0.99	0.36	3.72		4.68	4.43	1.13		1.19		3.32		0.36			
HP	0.12	0.30	3.45		2.98	2.75	1.07		1.15		3.00					
JD		0.26	2.39		2.29	1.94	1.04		1.16		2.97	4.76	9.85	3.19	2.95	
YS1	0.17	0.39	6.88		2.87	4.57	1.29		1.19		3.81	6.04	5.72	2.13	1.84	
YS2	0.16	0.39	4.19		2.83	2.26	2.69	0.67	4.24	0.76	5.35	0.53	0.66	1.55	0.38	
DD1		0.29	0.25	1.33	4.46	3.20			2.39	1.06		1.29	2.29	0.79	0.85	
DD2	0.17	0.35	0.31	4.38	4.31	3.23		1.74	2.75	1.11	1.82	2.10	1.53	2.68	0.81	
DD3	0.26	0.39	0.47	3.73	6.16	11.79		0.79		0.91	0.67		0.38			
DD4		0.26	0.31		1.98					0.87						
DL3	0.17	0.35	0.26	4.38	3.29	1.89				0.76			0.37	0.50		
DL5		0.30	0.28		4.44	1.97				0.69						
YT5	0.13	0.42	3.16		4.12	4.75	1.33				2.95			0.51		
YT6	0.93	0.32	3.78	3.60	4.72	5.68	1.35		1.02		4.39	1.01	0.72	1.45	0.32	
WH1	0.58	0.62	1.14	19.93	21.19	22.57	1.38		1.46	0.39	4.49	1.04	1.03	1.32	0.56	
WH2		0.35	3.25		2.83	3.22	1.25		1.20		3.01					
WH3	0.30	0.46	2.20		4.27	4.35	1.89		2.60	0.48	10.15	2.99	3.49	0.95	1.74	
QD1	1.24	1.64	1.49	6.99	17.97	14.31			4.79	1.51	1.53	2.60	2.25	4.19	1.06	
QD2		0.26	0.58		1.57				2.20	1.00						
QD3	0.96	0.30	0.35	5.44	1.49		0.35		2.44	1.36	6.33	1.33	1.36	1.14	0.54	
QD4		0.21	0.30	4.36	1.36				2.51	1.00		0.53		0.83		
QD5	0.20	0.55	2.90	3.72	4.25	4.49	0.93				2.31		0.45			
QD6	0.60	0.46	12.70	6.65	7.44	17.40	1.12		1.31	0.33	4.47	0.67	1.57	0.56	0.73	3.44
QD7	0.15	0.52	7.60		11.48	22.55	1.01		1.03		2.83		0.35			
RZ1	0.12	0.49	3.62	4.77	4.77	5.19	1.13				2.97		0.40			
RZ2	0.12	0.39	3.84	4.61	16.18	7.27	1.07				3.24		0.36			
LY1		0.28	2.14		3.19	2.77	1.16		1.04	0.35	2.70					
LY2		0.41	3.90		3.67	3.78	1.49		1.41	0.47	3.77		0.47	0.51		
LY3	0.47	0.47	5.80	4.97	5.97	7.28	1.14		1.05		2.59					
LY4			0.53				1.27		1.33	0.42	2.65					
YC1		0.45	2.83		4.46	2.32	1.19		1.33	0.41	2.66					
YC2		0.40	2.15		3.89	2.57	1.90		2.27	0.75	6.74	1.65	2.16	2.26	0.71	
YC3	0.22	0.46	5.49	6.73	6.85	5.93	2.24	1.29	1.85	0.50	7.24	1.71	1.71	6.78	2.51	
YC4		0.58	1.92		5.26	7.42	2.27		1.59	0.40	5.39		0.94		0.44	
YC5	0.83	0.34	2.86		3.27	2.42	1.58				3.22					
YC6	0.82	0.92	8.83	19.50	11.46	2.17	4.43	1.20	7.52	0.75	7.45	6.13	1.22	3.79	0.61	1.16
YC7		0.55	4.64		4.63	3.82	1.57		1.01		3.50					
YC8	0.88	0.29	2.38		2.62	2.48	1.56				2.90					
NT1	0.44	0.52	5.80	6.58	4.83	6.48	2.18	1.02	1.65	0.41	7.00		1.07	0.59		
NT2	0.21	0.54	5.86	3.62	6.82	5.12	1.60		1.14	0.29	3.66		0.59			
NT3	0.19	0.49	4.72	4.69	6.74	3.35	2.07		2.26		4.04	0.55	0.33			

Table S6. (Continued)

Sites	APs						SOs									
	OP	OP1EO	OP2EO	NP	NP1EO	NP2EO	SD1	SD2	SD3	SD4	ST1	ST2	ST3	ST4	ST5	ST6
NT4		0.26	2.55		1.87	2.58	2.21		1.30		4.10					
NT5	0.14	0.55	5.43		4.44	4.82	2.08	1.06	1.40	0.46	4.75			1.47	0.36	
NT6		0.38	2.22		3.60	2.33	1.94		1.50		4.39		0.36			
NT7		0.28	2.76		2.23	2.29	2.18	1.43	1.36	0.34	5.30		0.32	1.15	0.34	
NT8	0.16	0.62	4.65		8.35	3.62	2.14	1.02	1.43	0.32	5.77		0.31	1.34	0.44	
NT9	0.98	1.79	39.25	5.13	7.57	12.16	3.01	1.92	3.44	0.91	6.75	2.86	2.14	7.23	0.51	
NT10	0.49	0.60	8.81	7.68	14.80	25.25	15.57	1.97	17.22	1.97	92.22	7.19	14.17	4.35	4.87	4.13
DL1	0.18	0.33	0.36		1.53					1.17	1.34	1.99	2.77	2.42	0.96	1.26
DL2		0.26	0.26		1.48					0.88						
DL4	0.17	0.35	0.26	4.38	3.29	1.89				0.76			0.37	0.50		
DL6		0.30	0.28		4.44	1.97				0.69						
YK1	0.12	0.29	0.20	6.46	2.86	1.78				0.83		1.49	1.62	4.51	3.47	
YK2		0.35	0.25		2.43					0.83		0.54	0.53	0.80		
YK3		0.23	0.22		1.53					0.75		0.67	0.72	0.83	0.35	
PJ1	0.36	0.33	0.33	14.46	7.00	4.93			1.47	0.75	0.60	0.92	1.02	2.34	0.44	
PJ2	0.14	0.40	0.18	4.56	3.53				1.31	0.52			1.05	2.92	1.28	
JZ1		0.31	0.26		1.63					0.66			0.52	0.82		
JZ2		0.22	0.27		1.52					0.76			0.47	0.71		
JZ3		0.24	0.22		1.51		0.41			0.69	1.03		0.36			
JZ4		0.28	0.27		2.72					1.14	0.57	2.76	4.13	2.01	1.76	
JZ5		0.30	0.22		2.23	2.49		1.01		0.65			0.55	0.67	0.32	
HL1		0.36	0.52		2.93					0.65			0.61	0.95		
HL2		0.36	0.52		2.93			1.12	1.27	0.85		0.89	0.90	1.06	0.40	
HL3		0.15	0.17		1.69					0.86			0.47			
HL4	1.97	2.44	6.12	12.90	281.79	18.56		2.51	6.83	9.55	3.45	43.37	88.14	28.58	33.13	2.57
HL5		0.25	0.23		1.75	2.62			1.15	0.90			0.50	0.63		
HL6		0.27	0.44		2.11				1.48	1.13			0.38	0.59	0.38	
QH1		0.21	0.16		1.26				4.79	1.51	1.53	2.60	2.25	4.19	1.06	
QH2	0.18	0.27	0.17		1.80				1.01	0.73						
QH3	0.61	1.94	0.60	111.15	34.81	7.74		1.05	4.75	1.35	1.73	2.53	2.47	4.83	1.58	1.71
QH4	0.34	0.42	0.47	38.24	32.35	6.58			4.44	1.18	1.39	0.89	0.95	1.63	0.55	
QH5		0.26	0.36		2.16		1.69		12.48	1.25	4.62	1.27	1.79	4.94	1.53	
QH6	0.62	0.67	0.89	31.49	16.78	7.18	1.89	0.79	18.14	1.53	5.77	7.36	3.12	57.88	2.09	2.26
QH7	0.41	0.76	1.00	7.35	21.78	3.11			1.84	0.90		1.78	0.35	3.64		2.26
TS1		0.28	0.30		1.73	3.74			3.04	0.81	0.82		0.65	0.70	0.51	
TS2		0.13	0.15		0.75				3.15	0.90			0.42			
TS3		0.33	0.34		6.44	1.99			2.25	0.72		1.83	0.45	3.28		
TS5		0.26	0.19		2.78				1.53	0.74	0.62					
TS6		0.46	0.50		6.13	2.92			2.74	0.93			0.46	0.53		
TS7	0.24	0.53	0.90	11.18	8.14	6.40			11.23	1.65	2.56	3.20	4.33	2.72	1.60	3.22
TJ1		0.11	0.92		0.76		1.46		1.81	0.62	3.86	0.65	0.93	0.82	0.35	
TJ2	0.84	0.31	5.26	3.77	4.72	4.99	1.58		1.81	0.60	3.86		0.46	0.59		
TJ3		0.35	3.17		2.56	3.66	1.54	1.82	2.30	3.37	4.52	4.46	5.93	2.69	2.03	
TJ4	0.82	0.31	4.42		3.97	5.25	1.73		3.15	0.66	4.85	0.68	1.26	1.00	0.53	
TJ5		0.25	3.25		2.93	3.37	1.41		1.40	0.64	4.04	0.99	1.33	2.25	0.53	
TJ6		0.32	5.76	5.59	5.74	4.91	1.72		4.48	0.56	10.73		0.49			
TJ7		0.36	3.78		2.59	4.26	1.55		1.23	0.35	4.04		0.44			
BZ1		0.27	4.30		2.80	5.94	1.21		1.86	0.46	4.55	0.90	2.10	0.90	0.84	
BZ2	0.78	0.42	5.15		8.73	6.00	1.20		1.21	0.34	3.25	0.54	1.34		0.53	
BZ3		0.43	5.94		5.12	6.14	1.53		1.51	0.65	3.46	0.68	1.35	0.73	0.53	
BZ4	0.29	1.20	5.39	5.49	8.66	6.63	1.42		1.50	0.90	3.56		1.00	0.73	0.42	
BZ5		0.44	4.49		2.49	3.54	1.10		1.34	0.48	2.26	0.59	1.60	0.51	0.54	
BZ6		0.29	2.42		1.73	2.47	1.15			0.38	2.85	0.77	1.61	0.82	0.62	
DY1	0.11	0.26	3.32		2.74	4.77	1.42		1.07	0.35	19.53	1.23	2.73	1.21	0.87	
DY2	0.16	0.71	4.35		5.56	6.46	1.44		0.95	0.45	2.68	1.43	3.29	1.37	1.12	

Table S6. (Continued)

Sites	APs						SOs									
	OP	OP1EO	OP2EO	NP	NP1EO	NP2EO	SD1	SD2	SD3	SD4	SD5	SD6	SD7	SD8	SD9	SD10
DY3		0.27	3.34		2.34	4.48	1.14			0.35	2.56		0.81			
DY4		0.45	3.59		3.47	4.65	1.56		1.01	0.40	4.08	4.50	7.73	3.36	2.74	
DY5	0.17	0.39	11.93	6.22	18.42	2.46	2.41		23.32	0.67	6.06	1.68	2.80	6.48	1.15	1.48
WF1	0.14	0.44	3.96	4.50	4.39	5.96	1.36			0.34	3.76		0.53			
WF2	0.97	0.36	3.42	4.69	3.58	4.24	1.69		1.18		8.23	0.94	1.66	0.59	0.64	4.54
WF3	0.19	0.36	4.63	12.17	1.36	8.42	1.95		0.99	0.33	5.06	2.03	4.56	9.54	1.75	1.14
WF4	0.14	0.26	4.80		3.11	4.86	1.31			0.29	3.02	1.22	2.84	1.14	0.96	
WF5		0.38	2.53		3.59	4.89	1.34				2.68	0.94	2.19	0.89	0.70	
WF6	0.22	0.43	4.90	8.57	8.25	8.76	1.54		1.57		3.72	1.39	2.79	1.12	0.93	
WF7	0.11	0.42	3.27	4.40	4.60	4.67	1.06			0.30	2.30	1.26	2.70	1.21	0.92	
WF8	0.86	0.27	2.85		3.50	4.99	2.52		1.59	0.79	9.41	3.50	1.55	0.60	0.67	
YT1		0.30	2.83		2.58	3.25	1.50		1.00	0.33	4.09	0.78	1.52	1.03	0.51	
YT2	0.13	0.29	5.77	4.99	5.15	9.39	1.93	3.60	5.25	3.33	6.93	0.73	0.49	0.86	0.32	
YT3		0.39	2.18	4.33	3.87	3.49	1.60				4.02					
YT4	0.77	0.37	2.37	3.64	3.96	3.70	1.49		1.02		2.86	1.35	3.86	3.40	2.81	

Table S7. Fractional condition to identified sources (%) from base run using positive matrix factorization receptor model.

	Flu	Phe	Ant	Fl	Py	BaA	Chr	BbF	BkF	BaP	IcdP	DbahA	BghiP
Factor 1 – diesel & gasoline combustion	7	32	46	40	40	59	60	68	65	66	66	55	65
Factor 2 – biomass combustion	34	41	23	46	46	25	21	16	17	16	2	0	17
Factor 3 – coke oven	43	27	16	6	7	5	9	0	3	2	9	45	2
Factor 4 – others	16	0	16	7	7	11	10	16	16	16	12	0	16

Table S8. Statistical relationships of landuse type on persistent toxic substances (PTSs), for all PTS categories and by region. The bold text highlights statistically significant relationships.

Sea	Country	PTSs	Kruskal-Wallis test		*Post hoc* Mann-Whitney (*P* values)[a]						
			F-value	P value	I-A	I-B	I-Ba	M-A	M-B	M-S	M-Ba
All	All	PAHs	54.3	**<0.001**	**0.001**	**<0.001**	**<0.001**	**<0.001**	**<0.001**	0.616	**<0.001**
		APs	10.9	0.146							
		SOs	16.2	**0.015**	0.196	0.251	0.554	1.000	1.000	1.000	1.000
Yellow Sea	Korea	PAHs	1.44	0.676							
		APs	5.80	0.128							
		SOs	4.27	0.227							
	China	PAHs	26.9	**<0.001**	0.324	**0.023**	**0.002**	0.346	**0.025**	-[b]	**0.002**
		APs	10.5	0.061							
		SOs	11.0	0.052							
Bohai Sea	China	PAHs	36.4	**<0.001**	**0.030**	**0.010**	**0.001**	**0.005**	**0.025**	**0.023**	**<0.001**
		APs	1.22	0.934							
		SOs	5.82	0.571							

[a] I-Industrial; M-Municipal; A-Agricultural; B-Beach; Ba-Barren; S-Saltern

[b] Post-hoc test not conducted.

Table S9. Statistical relationships of regional differences, by land use type. The bold text highlights statistically significant relationships.

Landuse type	PTSs	Kruskal-Wallis test		*Post hoc* Mann-Whitney (*P* values)		
		F-value	P value	Y-K[a] *vs* Y-C[b]	Y-K *vs* B-C[c]	Y-S *vs* B-C
Industrial	PAHs	7.52	**0.023**	**0.029**	**0.035**	1.000
	APs	3.46	0.178			
	SOs	4.06	0.132			
Municipal	PAHs	5.40	0.067			
	APs	0.67	0.714			
	SOs	2.03	0.363			
Agricultural	PAHs	4.70	0.095			
	APs	0.34	0.842			
	SOs	0.13	0.937			
Beach	PAHs	0.43	0.805			
	APs	6.06	**0.048**	**0.048**	0.295	1.000
	SOs	0.16	0.924			
Barren[d]	PAHs					0.545
	APs					0.880
	SOs					0.390

[a] Y-K: Yellow Sea-Korea

[b] Y-C: Yellow Sea-China

[c] B-C: Bohai Sea-China

[d] n = 2 (Yellow Sea-China and Bohai Sea-China)

Table S10. Statistical relationships (Spearman rank) of regional differences between PTSs and physicochemical parameters in sediments, by land use type and region for the Yellow and Bohai seas. Bold text highlights statistically significant relationships.

PTSs	Physicochemical parameters	Yellow Sea-Korea			Yellow Sea-China						Bohai Sea-China					
		Industrial	Agricultural	Beach	Industrial	Municipal	Agricultural	Beach	Aqua[a]	Barren	Industrial	Municipal	Agricultural	Beach	Saltern	Barren
PAHs	Mud content	0.50	**0.69***	0.00	-0.20	0.31	0.21	**1.00****	0.54	0.18	0.25	0.09	0.39	0.87	-0.32	-0.14
	TN	**1.00****	**0.69***	0.00	-0.15	0.17	**0.90****	0.87	0.60	0.20	-0.58	0.64*	**0.82****	0.87	0.95	0.13
	TOC	**1.00****	**0.87****	-0.50	-0.03	0.37	**0.79***	**1.00****	0.43	0.33	0.48	0.42	**0.68****	-0.50	0.95	0.22
	C/N	**1.00****	-0.16	0.00	0.54	0.37	0.43	-0.50	-0.14	0.37	-0.29	-0.20	0.30	-0.50	0.32	0.32
	$\delta^{13}C$	0.50	-0.18	-0.50	0.31	0.60	0.75	-0.50	-0.43	0.12	0.21	0.54	-0.07	-0.50	0.32	0.22
APs	Mud content	**1.00****	**0.59***	**1.00****	0.14	0.31	-0.18	0.50	0.43	0.44	-0.12	-0.03	-0.01	**-1.00****	-0.40	**0.56***
	TN	0.50	**0.80****	**1.00****	0.03	0.23	-0.02	1.00	0.49	0.42	0.20	0.60*	0.20	**-1.00****	**1.00****	0.53
	TOC	0.50	**0.76****	0.87	0.09	0.03	-0.29	0.67	0.66	0.15	0.16	0.65*	0.19	0.01	**1.00****	**0.61***
	C/N	0.50	-0.01	**1.00****	0.43	0.03	-0.57	0.67	0.26	0.22	-0.49	0.04	0.08	0.01	0.20	0.10
	$\delta^{13}C$	**1.00****	-0.28	0.87	0.09	0.54	0.46	0.67	-0.14	0.29	-0.15	0.40	0.01	0.87	0.40	-0.16
SOs	Mud content	0.50	0.53	0.87	-0.03	0.26	0.14	**1.00****	0.78	-0.09	-0.14	-0.38	0.13	-0.87	-0.20	**0.56***
	TN	**1.00****	0.27	0.87	-0.27	0.15	0.40	0.87	0.78	-0.15	0.01	0.22	0.14	-0.87	0.80	0.27
	TOC	**1.00****	0.12	0.50	-0.66	0.09	0.21	**1.00****	0.78	-0.31	0.25	0.19	0.16	-0.50	0.80	0.14
	C/N	**1.00****	-0.01	-0.87	0.14	0.09	-0.14	-0.50	0.27	-0.05	-0.21	-0.22	0.06	-0.50	0.40	-0.08
	$\delta^{13}C$	0.50	0.09	0.50	0.37	0.37	0.68	-0.50	-0.68	-0.41	-0.13	0.53	**0.59****	**1.00****	0.20	0.26

[a] Aqua: Aquaculture

[*] Significantly correlated at $p < 0.05$ level (2-tailed).

[**] Significantly correlated at $p < 0.01$ level (2-tailed).

Supplementary Figures

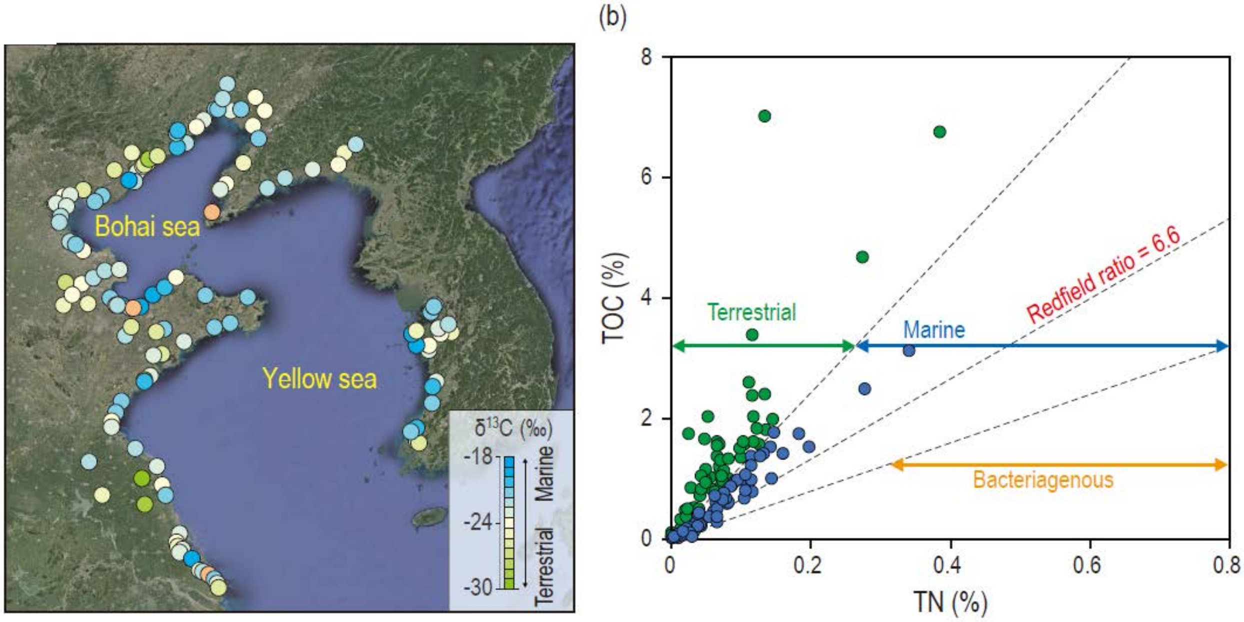

Fig. S1. (a) Spatial distribution of δ^{13}C values and (b) C/N ratios in the sediment of Yellow and Bohai seas.

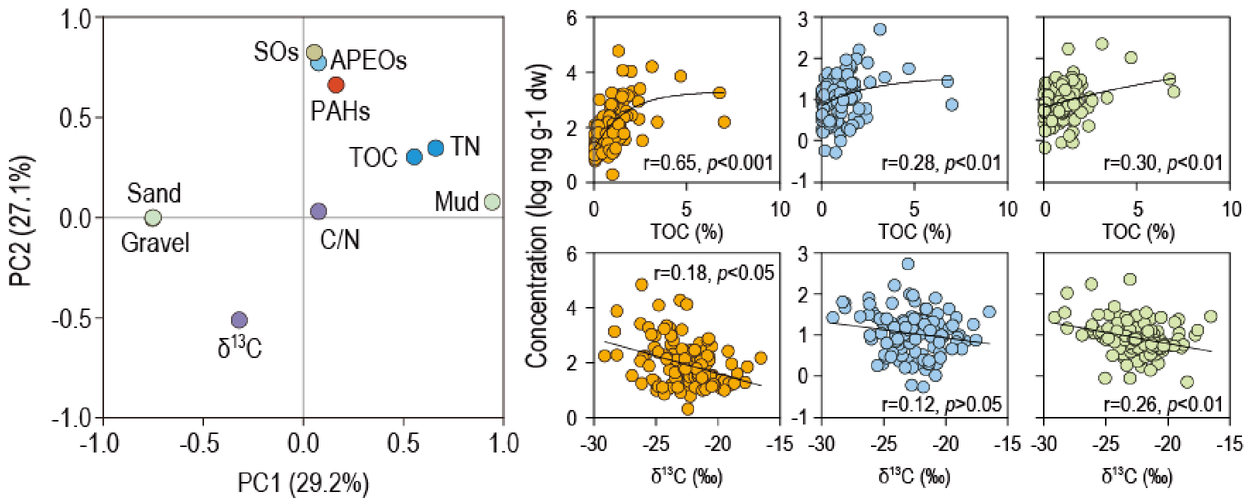

Fig. S2. Relationships among PTSs. Panels: (left) Principal Component Analysis (PCA) ordination of PTSs and physicochemical parameters and (right) the relationship between PTSs and TOC or $\delta^{13}C$.

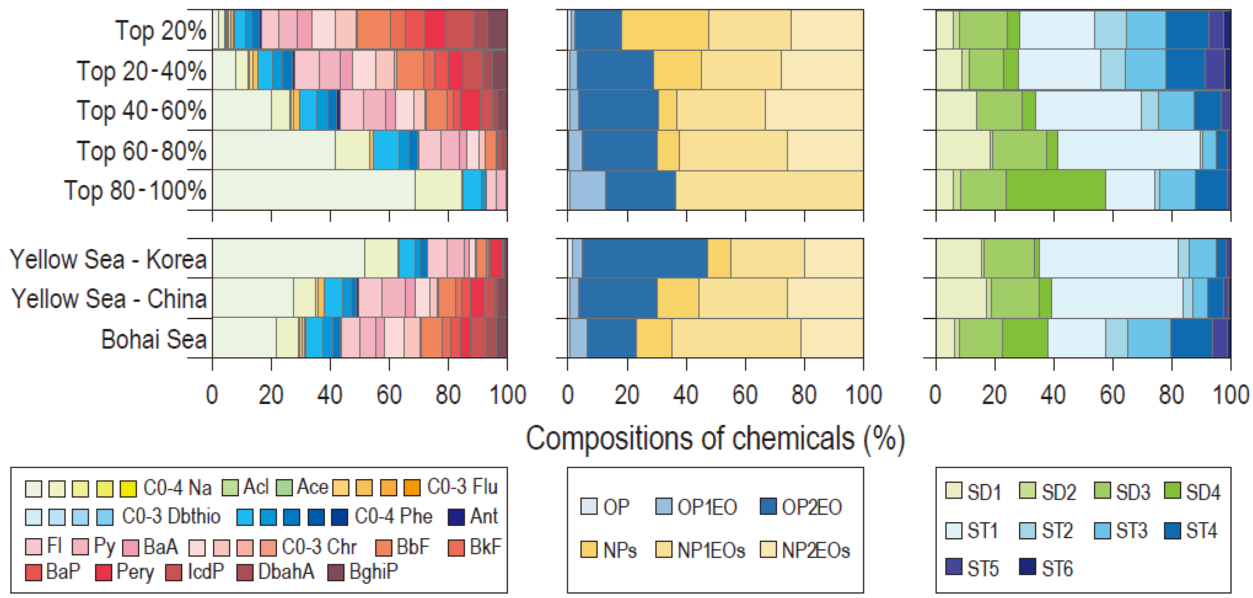

Fig. S3. Composition of PTSs among concentration groups, by concentration (20% interval of concentrations) and region.

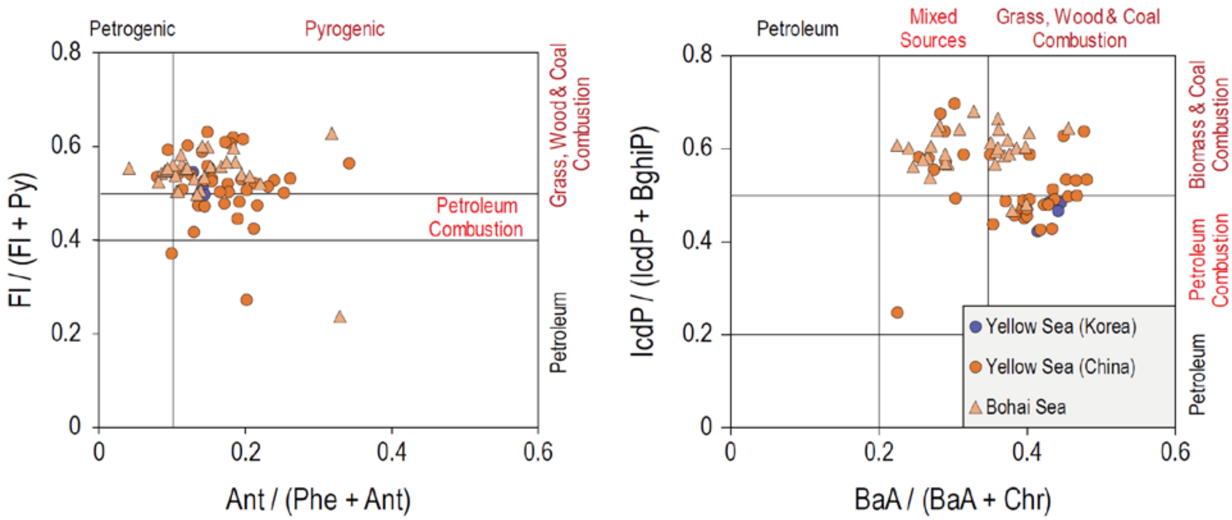

Fig. S4. Diagnostic ratios for prediction of PAHs sources between Ant/(Ant+Phe) and Fl/(Fl+Py), and BaA/(BaA+Chr) and IcdP/(IcdP+BghiP).

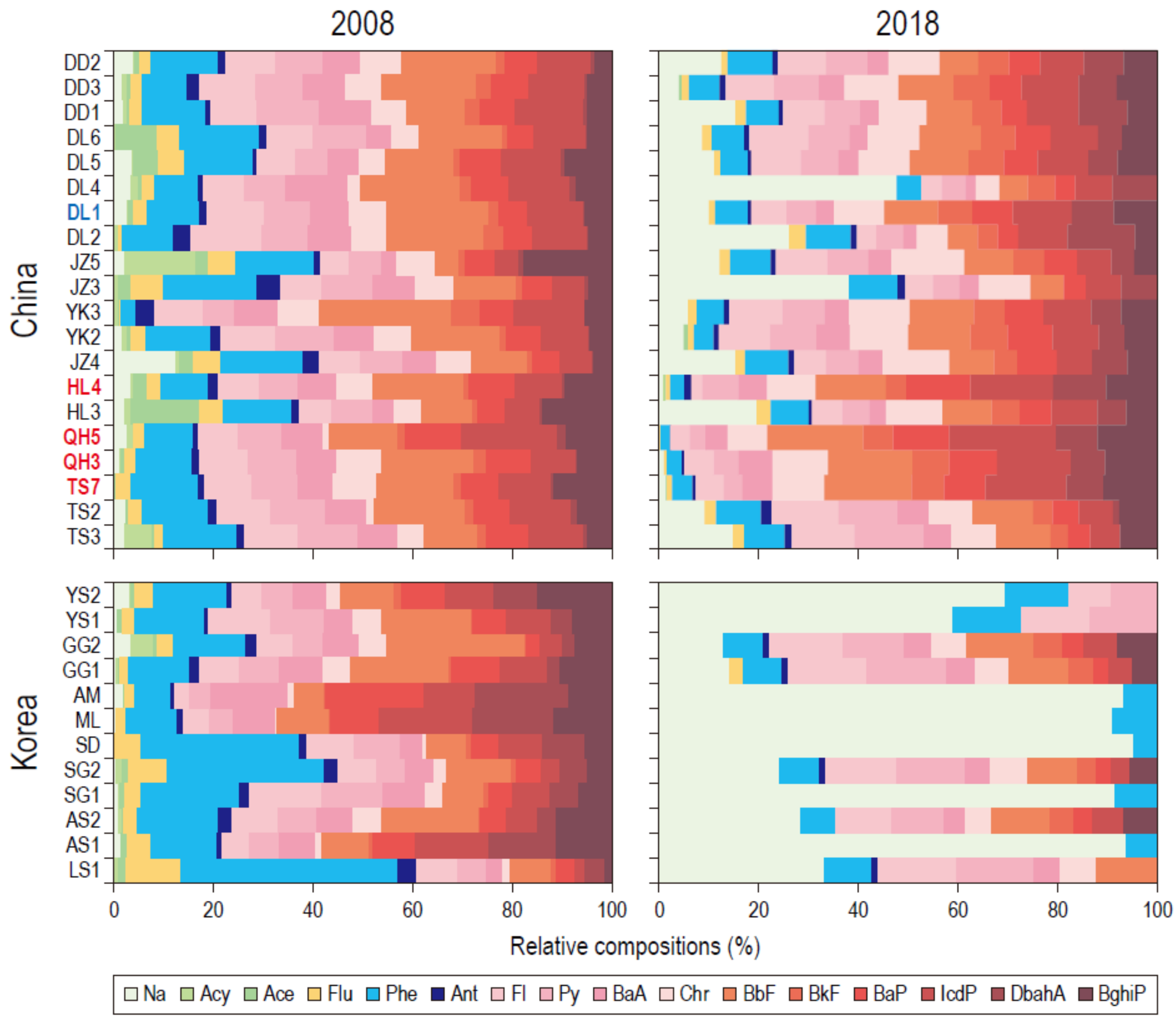

Fig. S5. Compositions of 16 PAHs in 2008 and 2018 in sediments of the Yellow and Bohai seas.